

Resummation of threshold double logarithms in quarkonium fragmentation functions

Hee Sok Chung,^{1,2,*} U-Rae Kim,^{3,†} and Jungil Lee^{2,‡}

¹*Department of Mathematics and Physics,*

Gangneung-Wonju National University, Gangneung 25457, Korea

²*Department of Physics, Korea University, Seoul 02841, Korea*

³*Department of Physics, Korea Military Academy, Seoul 01805, Korea*

(Dated: February 16, 2026)

Abstract

We develop a formalism for resumming threshold double logarithms that appear in fragmentation functions for production of heavy quarkonia. Threshold singularities appear in fixed-order calculations of quarkonium fragmentation functions in the nonrelativistic QCD factorization formalism due to radiation of soft gluons. Because of this, at fixed order quarkonium fragmentation functions are not positive definite, and can lead to unphysically negative cross sections. This problem can be resolved by resumming threshold logarithms to all orders in perturbation theory, which renders the fragmentation functions finite and ensures the positivity of cross sections. We present a detailed derivation of the resummation formalism and derive the formula for resummed quarkonium fragmentation functions, which can be computed entirely within perturbation theory without the need for nonperturbative model functions.

I. INTRODUCTION

It has been known for a long time that short-distance hadronic cross sections involve large corrections from radiation of soft gluons, which can be resummed by exponentiation [1–15]. In fixed-order perturbation theory, the soft-gluon corrections produce logarithmic singularities that spoil the convergence of the perturbative expansion near the boundaries of phase space. As the strongest singularities of this type appear as double logarithms, they are commonly referred to as threshold double logarithms. These logarithms can be resummed to all orders in perturbation theory with the help of perturbative factorization, and only then the cross sections become finite and smooth near the threshold.

It has also been known that fragmentation functions for production of quarkonia, when computed in the nonrelativistic QCD (NRQCD) factorization formalism [16], involve singularities of similar nature. The appearance of threshold double logarithms in quarkonium fragmentation functions was first discovered by Braaten and Lee in the next-to-leading order (NLO) calculation of the color-octet 3S_1 gluon fragmentation function for heavy quarkonium in Ref. [17]. Later, threshold double logarithms were also found in the NLO calculation of P -wave fragmentation functions in Ref. [18]. Because these singularities are associated with

* heesokchung@gwnu.ac.kr

† kim87@kma.ac.kr

‡ jungil@korea.ac.kr

radiation of soft gluons, quarkonium fragmentation functions computed in fixed-order perturbation theory involve distributions that become increasingly singular at the kinematical threshold with increasing order in the strong coupling. For some time these singularities in fragmentation functions have been considered not much more than a technical nuisance that requires some care when computing cross sections [19, 20], as they are integrable and do not produce actual divergences in sufficiently inclusive observables such as transverse-momentum-dependent cross sections. This conventional viewpoint faced a serious challenge when it was found that quarkonium production rates computed at NLO accuracy can turn unphysically negative at very large transverse momentum. This happens because the threshold double logarithmic singularities in fragmentation functions can indeed produce dynamical effects in production rates, because they produce radiative corrections of the form $\alpha_s \log^2 p_T$, where α_s is the strong coupling and p_T is the transverse momentum of the heavy quarkonium. This lead to an effort to theoretically understand the threshold logarithms in quarkonium fragmentation functions to all orders in perturbation theory [21, 22], so that measurements of large- p_T production rates of J/ψ in Ref. [23] could be well described in QCD.

The first complete calculation of resummation of threshold double logarithms in inclusive hadroproduction rates of heavy quarkonium was presented in Ref. [24]. Similarly to the case of hadronic cross sections in perturbative QCD, after resummation the quarkonium fragmentation functions no longer involve singularities at the kinematical threshold. Because of this, at least for some choice of NRQCD long-distance matrix elements, it is possible to construct quarkonium fragmentation functions that are positive definite over the whole kinematically allowed region, which ensures positivity of production cross sections. In contrast, this is impossible in fixed-order perturbation theory, because the singularities produce distributions that change sign rapidly at the kinematical end point. Hence, only after threshold resummation can the large- p_T production rates of heavy quarkonia be under theoretical control.

In this paper, we present the detailed derivation of the threshold resummation formalism used in Ref. [24]. The formalism is based on standard methods of perturbative factorization in QCD, such as the Grammer-Yennie approximation [25] that systematically isolates the source of infrared singularities of Feynman diagrams in gauge theories. This leads to a soft factorization of the quarkonium fragmentation function in terms of soft functions, which completely contain the threshold singularities in the fragmentation function. The threshold

singularities in the soft functions take an especially simpler form at the double logarithmic level, which allows an all-orders resummation by exponentiation. This results in fragmentation functions that are free of threshold singularities, and are smooth and well behaved at the kinematical end point, similar to nonperturbative model functions used to describe fragmentation functions for single inclusive hadron production.

This paper is organized as follows. In Sec. II we collect the known results for fixed-order calculations of quarkonium fragmentation functions in the NRQCD factorization formalism. In Sec. III we derive the soft factorization formulas for quarkonium fragmentation functions. The validity of soft factorization is then verified at leading nonvanishing order in the strong coupling in Sec. IV. In Sec. V we compute the soft functions at NLO in the strong coupling, and identify the source of the double logarithmic singularities at threshold. Based on the NLO results of the soft functions, the resummation formula for threshold double logarithms in quarkonium fragmentation functions are derived in Sec. VI. We conclude in Sec. VII.

II. THRESHOLD LOGARITHMS IN QUARKONIUM FRAGMENTATION FUNCTIONS

A. NRQCD factorization

In the NRQCD factorization formalism [16], the transverse-momentum-dependent inclusive production rates of a heavy quarkonium \mathcal{Q} at large transverse momentum p_T is described by the factorization formula

$$\frac{d\sigma_{\mathcal{Q}}}{dp_T} = \sum_{\mathcal{N}} \frac{d\sigma_{Q\bar{Q}(\mathcal{N})}}{dp_T} \langle \mathcal{O}^{\mathcal{Q}}(\mathcal{N}) \rangle, \quad (1)$$

where the short-distance coefficient (SDC) $d\sigma_{Q\bar{Q}(\mathcal{N})}/dp_T$ corresponds to the p_T -differential cross section of a heavy quark Q and an antiquark \bar{Q} pair in a specific color and angular momentum state \mathcal{N} , and $\langle \mathcal{O}^{\mathcal{Q}}(\mathcal{N}) \rangle$ is the NRQCD long-distance matrix element (LDME) that describes the nonperturbative evolution of the $Q\bar{Q}$ in the state \mathcal{N} into a quarkonium \mathcal{Q} plus light particles. The sum over \mathcal{N} is usually truncated at a chosen accuracy in the nonrelativistic expansion; for the P -wave quarkonia such as $\mathcal{Q} = \chi_{cJ}$ with $J = 0, 1$, and 2 the ${}^3P_J^{[1]}$ and ${}^3S_1^{[8]}$ channels appear at leading order in the nonrelativistic expansion, while for S -wave quarkonia such as $\mathcal{Q} = J/\psi$ or $\psi(2S)$ the ${}^3S_1^{[1]}$, ${}^3S_1^{[8]}$, ${}^1S_0^{[8]}$, and ${}^3P_J^{[8]}$ channels give dominant contributions to the cross section.

The SDCs can be computed perturbatively. At large p_T , we can compute the SDCs in the leading-power (LP) fragmentation formalism [26, 27]

$$\frac{d\sigma_{Q\bar{Q}(\mathcal{N})}^{\text{LP}}}{dp_T} = \sum_{i=g,q,\bar{q}} \int_0^1 dz \frac{d\hat{\sigma}_{i(K)}}{dp_T} D_{i \rightarrow Q\bar{Q}(\mathcal{N})}(z), \quad (2)$$

where $\hat{\sigma}_{i(K)}$ is the cross section for production of a massless parton $i = g$, q , or \bar{q} with momentum K , $D_{i \rightarrow Q\bar{Q}(\mathcal{N})}(z)$ is the fragmentation function (FF) for fragmentation of a parton i into $Q\bar{Q}(\mathcal{N})$, $z = P^+/K^+$ is the fraction of the $Q\bar{Q}$ momentum P along the $+$ direction, which is taken to be the direction of P in the lab frame. Both the $\hat{\sigma}_{i(K)}$ and the FFs $D_{i \rightarrow Q\bar{Q}(\mathcal{N})}(z)$ are available to NLO accuracy¹, which allow computation of the SDCs to NLO at large p_T . The validity of Eq. (2) is based on the collinear factorization theorem of QCD, which is the foundation of all first-principles calculation of single inclusive hadron production at large transverse momentum; for heavy quarkonium production in NRQCD, the formula has been tested numerically up to $p_T = 400$ GeV at NLO accuracy [20, 29]. Corrections to Eq. (2), which are suppressed by m^2/p_T^2 with m the heavy quark mass, are given in terms of next-to-leading-power (NLP) factorization.

The $D_{i \rightarrow Q\bar{Q}(\mathcal{N})}(z)$ in Eq. (2) can be computed perturbatively from the Collins-Soper definition for the FFs [26]. When computed in fixed-order perturbation theory, the FFs involve distributions that are singular at threshold $z = 1$ such as plus distributions or the delta function $\delta(1 - z)$, because there are diagrams where a $Q\bar{Q}$ are produced from a gluon after radiation of a fixed number of soft gluons, or even without emitting any partons at all. Because the singularities in the FFs are integrable, and the parton production cross sections $d\hat{\sigma}_{i(K)}$ are regular functions in z , the cross sections $d\sigma_{Q\bar{Q}(\mathcal{N})}^{\text{LP}}$ are finite despite these singularities. However, the singularities do affect the cross sections because the $d\hat{\sigma}_{i(K)}$ steeply rise as $z \rightarrow 1$ as a power in z , which makes the $d\sigma_{Q\bar{Q}(\mathcal{N})}^{\text{LP}}$ very sensitive to the behavior of the FFs near threshold². This problem is especially important in hadroproduction, because the steep rise of the $d\hat{\sigma}_{i(K)}$ in z becomes stronger with increasing p_T , due to the decrease of parton densities in the initial state. Hence, the singular behavior of the FFs affect the p_T shapes of the cross sections $d\sigma_{Q\bar{Q}(\mathcal{N})}^{\text{LP}}$.

¹ Very recently, next-to-next-to-leading order calculation of the parton production cross sections has been reported in Ref. [28].

² Note that this problem is not so severe in calculation of single inclusive production rates of light hadrons, because in such calculations the nonperturbative model functions for the FFs are taken to be regular functions in z that usually vanish as $z \rightarrow 1$.

Explicit calculations of the FFs $D_{i \rightarrow Q\bar{Q}(\mathcal{N})}(z)$ at NLO accuracy show that the strongest of the singularities at NLO appear as *threshold double logarithms*, which are proportional to $\alpha_s \left[\frac{\log(1-z)}{1-z} \right]_+ \otimes D^{\text{LO}}(z)$ [17, 18]. Here the convolution \otimes is defined by

$$(f \otimes g)(z) = \int_0^1 \frac{dz'}{z'} f(z') g(z/z'). \quad (3)$$

Appearance of threshold double logarithms in perturbative calculations of FFs has been known for a long time, such as in $D_{q \rightarrow q}(z)$ (see, for example, Ref. [5]). These singularities become more severe with increasing order in the strong coupling α_s , as they appear in the form $\alpha_s^n \left[\frac{\log^{2n-1}(1-z)}{1-z} \right]_+ \otimes D^{\text{LO}}(z)$. As threshold logarithms at higher orders in α_s will have increasingly stronger effects on the p_T shapes of the cross sections $d\sigma_{Q\bar{Q}(\mathcal{N})}^{\text{LP}}$, the cross sections computed in fixed-order perturbation theory will have very different p_T shapes depending on at which order the perturbation series has been truncated. Therefore, to obtain a proper theoretical description of large- p_T production rates of heavy quarkonia, it is imperative to understand the all-orders structure of threshold double logarithms in quarkonium FFs.

B. Threshold singularities in gluon fragmentation functions

We now summarize the threshold double logarithms that appear in NLO calculations of gluon FFs. The gluon FFs for the ${}^3S_1^{[8]}$, ${}^3P_J^{[8]}$, ${}^1S_0^{[8]}$, and ${}^3P_J^{[1]}$ channels to order- α_s^2 accuracy

are given by [17, 30–34]

$$D_{g \rightarrow Q\bar{Q}(^3S_1^{[8]})}(z) = \frac{\pi\alpha_s}{(d-1)(N_c^2-1)m^3} \left\{ \delta(1-z) + \frac{\alpha_s}{\pi} \left[A(\mu_R)\delta(1-z) \right. \right. \\ \left. \left. + \left(\log \frac{\mu_F}{2m} - \frac{1}{2} \right) P_{gg}(z) + \frac{3(1-z)}{z} \right. \right. \\ \left. \left. + 6(2-z+z^2)\log(1-z) - \frac{2N_c}{z} \left(\frac{\log(1-z)}{1-z} \right)_+ \right] \right\} + O(\alpha_s^3), \quad (4a)$$

$$D_{g \rightarrow Q\bar{Q}(^3P_J^{[8]})}(z) = \frac{8\alpha_s^2}{3(d-1)(N_c^2-1)m^5} \frac{N_c^2-4}{4N_c} \left[\left(\frac{1}{6} - \log \frac{\mu_\Lambda}{2m} \right) \delta(1-z) \right. \\ \left. + \frac{1}{(1-z)_+} + \frac{13-7z}{4} \log(1-z) - \frac{(1-2z)(8-5z)}{8} \right] + O(\alpha_s^3), \quad (4b)$$

$$D_{g \rightarrow Q\bar{Q}(^1S_0^{[8]})}(z) = \frac{\alpha_s^2}{8m^3} \frac{N_c^2-4}{4N_c} [3z-2z^2+2(1-z)\log(1-z)] + O(\alpha_s^3), \quad (4c)$$

$$D_{g \rightarrow Q\bar{Q}(^3P_J^{[1]})}(z) = \frac{2\alpha_s^2}{9N_c^2m^5} \left[\left(\frac{Q_J}{2J+1} - \log \frac{\mu_\Lambda}{2m} \right) \delta(1-z) \right. \\ \left. + \frac{z}{(1-z)_+} + \frac{P_J(z)}{2J+1} \right] + O(\alpha_s^3), \quad (4d)$$

where d is the number of spacetime dimensions, $N_c = 3$ is the number of colors, $A(\mu_R) = \frac{\beta_0}{2} \left(\log \frac{\mu_R}{2m} + \frac{13}{6} \right) + \frac{2}{3} - \frac{\pi^2}{2} + 8\log 2$, $\beta_0 = \frac{11}{3}N_c + \frac{2}{3}n_f$ is the QCD beta function at one loop, $P_{gg}(z) = 2C_A \left[\frac{z}{(1-z)_+} + \frac{1-z}{z} + z(1-z) + \frac{\beta_0}{12}\delta(1-z) \right]$ the gluon splitting function, $C_A = N_c$, and the J -dependent constants and functions are given by

$$Q_0 = \frac{1}{4}, \quad Q_1 = \frac{3}{8}, \quad Q_2 = \frac{7}{8}, \quad (5)$$

$$P_0(z) = \frac{z(85-26z)}{8} + \frac{9(5-3z)}{4} \log(1-z), \quad (6)$$

$$P_1(z) = -\frac{3z(1+4z)}{4}, \quad (7)$$

$$P_2(z) = \frac{5z(11-4z)}{4} + 9(2-z)\log(1-z). \quad (8)$$

The scales μ_R and μ_F come from the renormalization of the QCD coupling and the FF, respectively. The scale μ_Λ that appears in the P -wave FFs is the renormalization scale for the $^3S_1^{[8]}$ matrix element in the $\overline{\text{MS}}$ scheme. The explicit logarithmic dependence on μ_Λ appears in the P -wave FFs because the IR pole that arises from the phase space integral of the P -wave production process is canceled by the one-loop correction to the $^3S_1^{[8]}$ matrix element. The gluon FF for the $^3S_1^{[1]}$ state, which begins at order α_s^3 , has been obtained in Ref. [35] as an integral representation; later, an analytical result has been obtained in Ref. [36].

Note that the gluon FF for the ${}^3S_1^{[8]}$ state, as well as those for the ${}^3P_J^{[8]}$ and ${}^3P_J^{[1]}$ states, contain distributions that are singular at $z = 1$ at leading nonvanishing orders in α_s . Due to these singularities at the threshold, the cross sections $\sigma_{Q\bar{Q}(N)}$ are very sensitive to the behavior of the gluon cross sections $\hat{\sigma}_{g(K)}$ near $z = 1$. The severity of the singularities can be quantified through the Mellin transform. The definition of the Mellin transform and some useful formulas can be found in Appendix A. We see that while the $\delta(1 - z)$ term yields a nonzero constant in Mellin space, the Mellin transform of $1/(1 - z)_+$ diverges like $-\log N$, which makes the $z = 1$ singularity in the plus distribution a more severe one compared to the Dirac delta function. It is known that QCD radiative corrections exacerbate these singularities; for example, the most singular term in the N^n LO correction to the FF is proportional to

$$\left(\frac{\alpha_s}{\pi}\right)^n \left[\frac{\log^{2n-1}(1-z)}{1-z} \right]_+ \otimes D^{\text{LO}}(z), \quad (9)$$

where $D^{\text{LO}}(z)$ is the FF at leading nonvanishing order in α_s . As shown in Appendix A, the large- N asymptotic behavior of this term in Mellin space is

$$\int_0^1 \frac{dz}{z} z^N \left(\frac{\alpha_s}{\pi}\right)^n \left[\frac{\log^{2n-1}(1-z)}{1-z} \right]_+ \otimes D^{\text{LO}}(z) \sim \frac{1}{2n} \left(\frac{\alpha_s}{\pi} \log^2 N\right)^n \tilde{D}^{\text{LO}}(N), \quad (10)$$

which become more singular as n increases. As the leading logarithmic behavior is given by powers of $\alpha_s \log^2 N$, these singularities are called *threshold double logarithms*. Due to the appearance of threshold logarithms, the sensitivity to the behavior of the gluon cross section near $z = 1$ becomes stronger with increasing order in α_s , which calls for need to resummation.

In the case of the ${}^1S_0^{[8]}$ and ${}^3S_1^{[1]}$ channels, the gluon FFs are regular functions in z , meaning that the Mellin-space FFs vanish at least like $1/N$ as $N \rightarrow \infty$. While radiative corrections may involve logarithms in N , these logarithms will always be suppressed by at least a power of $1/N$. Hence, even at higher orders in α_s , the gluon FFs for these channels will not involve distributions that are singular at $z = 1$.

The appearance of threshold logarithms in quarkonium FFs has been confirmed explicitly from NLO calculations. NLO corrections to the gluon FFs have been computed for all ${}^3S_1^{[8]}$, ${}^3P_J^{[8]}$, ${}^1S_0^{[8]}$, and ${}^3P_J^{[1]}$ channels. The analytical result for the one-loop correction to $D_{g \rightarrow Q\bar{Q}({}^3S_1^{[8]})}(z)$ is shown in Eq. (4a). The radiative correction to $D_{g \rightarrow Q\bar{Q}({}^1S_0^{[8]})}(z)$, which

only contain regular functions in z , has been computed numerically [37, 38]. The order- α_s^3 correction to $D_{g \rightarrow Q\bar{Q}(^3P_J^{[8]})}(z)$ and $D_{g \rightarrow Q\bar{Q}(^3P_J^{[1]})}(z)$ have been computed semi analytically, where coefficients of plus distributions and the Dirac delta function are known exactly, while contributions from regular functions are known numerically [18]. The order- α_s^3 contribution to $D_{g \rightarrow Q\bar{Q}(^3P_J^{[1]})}(z)$ has the form

$$\begin{aligned} D_{g \rightarrow Q\bar{Q}(^3P_J^{[1]})}(z) \Big|_{\mu_R=\mu_F=\mu_\Lambda=2m} &= D_{g \rightarrow Q\bar{Q}(^3P_J^{[1]})}^{\text{LO}}(z) + \frac{2\alpha_s^2}{9N_c^2 m^5} \\ &\times \frac{\alpha_s}{\pi} \left[\sum_{n=0}^2 p_n^{J,[1]} \left(\frac{\log^n(1-z)}{1-z} \right)_+ + p_\delta^{J,[1]} \delta(1-z) + p^{J,[1]}(z) \right], \end{aligned} \quad (11)$$

where $D_{g \rightarrow Q\bar{Q}(^3P_J^{[1]})}^{\text{LO}}(z)$ is the order- α_s^2 contribution shown in Eq. (4d), while the order- α_s^3 contribution to $D_{g \rightarrow Q\bar{Q}(^3P_J^{[8]})}(z)$ has the form

$$\begin{aligned} D_{g \rightarrow Q\bar{Q}(^3P_J^{[8]})}(z) \Big|_{\mu_R=\mu_F=\mu_\Lambda=2m} &= D_{g \rightarrow Q\bar{Q}(^3P_J^{[8]})}^{\text{LO}}(z) + \frac{8\alpha_s^2}{3(d-1)(N_c^2-1)m^5} \frac{N_c^2-4}{4N_c} \\ &\times \frac{\alpha_s}{\pi} \left[\sum_{n=0}^2 p_n^{[8]} \left(\frac{\log^n(1-z)}{1-z} \right)_+ + p_\delta^{[8]} \delta(1-z) + p^{[8]}(z) \right], \end{aligned} \quad (12)$$

where $D_{g \rightarrow Q\bar{Q}(^3P_J^{[8]})}^{\text{LO}}(z)$ is the order- α_s^2 contribution shown in Eq. (4b). The coefficients of the $\left(\frac{\log^2(1-z)}{1-z} \right)_+$ term are independent of the color and J of the final state, and depends only on N_c :

$$p_2^{J,[1]} = p_2^{[8]} = -4N_c, \quad (13)$$

while the p_1 , p_0 , p_δ , and the regular functions $p(z)$ in general depend on J and the color. By taking the Mellin transform, we can find the large- N asymptotic behaviors of the $^3S_1^{[8]}$, $^3P_J^{[8]}$, and $^3P_J^{[1]}$ FFs given by

$$\tilde{D}_{g \rightarrow Q\bar{Q}(^3S_1^{[8]})}(N) \sim \frac{\pi\alpha_s}{(d-1)(N_c^2-1)m^3} \left[1 - \frac{\alpha_s N_c}{\pi} (\log^2 N + \dots) \right] + O(\alpha_s^3), \quad (14a)$$

$$\begin{aligned} \tilde{D}_{g \rightarrow Q\bar{Q}(^3P_J^{[8]})}(N) &\sim \frac{8\alpha_s^2}{3(d-1)(N_c^2-1)m^5} \frac{N_c^2-4}{4N_c} \left[-\log N + O(1/N^0) \right. \\ &\quad \left. + \frac{4}{3} \frac{\alpha_s N_c}{\pi} (\log^3 N + \dots) \right] + O(\alpha_s^4), \end{aligned} \quad (14b)$$

$$\tilde{D}_{g \rightarrow Q\bar{Q}(^3P_J^{[1]})}(N) \sim \frac{2\alpha_s^2}{9N_c^2 m^5} \left[-\log N + O(1/N^0) + \frac{4}{3} \frac{\alpha_s N_c}{\pi} (\log^3 N + \dots) \right] + O(\alpha_s^4), \quad (14c)$$

where the \dots represent terms that are less divergent than the preceding term. While the threshold double logarithm in the ${}^3S_1^{[8]}$ gluon FF is $-\frac{\alpha_s}{\pi} N_c \log^2 N$ times the leading-order piece, the threshold double logarithm in the P -wave FFs is $-\frac{4}{3} \frac{\alpha_s}{\pi} N_c \log^2 N$ times the leading-order piece for both ${}^3P_J^{[8]}$ and ${}^3P_J^{[1]}$ channels. That is, if we only collect the leading threshold double logarithms in the NLO correction, we can write

$$\tilde{D}_{g \rightarrow Q\bar{Q}({}^3S_1^{[8]})}(N) \sim \left(1 - \frac{\alpha_s N_c}{\pi} \log^2 N + O(\alpha_s^2)\right) \tilde{D}_{g \rightarrow Q\bar{Q}({}^3S_1^{[8]})}^{\text{LO}}(N), \quad (15a)$$

$$\tilde{D}_{g \rightarrow Q\bar{Q}({}^3P_J^{[8]})}(N) \sim \left(1 - \frac{4}{3} \frac{\alpha_s N_c}{\pi} \log^2 N + O(\alpha_s^2)\right) \tilde{D}_{g \rightarrow Q\bar{Q}({}^3P_J^{[8]})}^{\text{LO}}(N), \quad (15b)$$

$$\tilde{D}_{g \rightarrow Q\bar{Q}({}^3P_J^{[1]})}(N) \sim \left(1 - \frac{4}{3} \frac{\alpha_s N_c}{\pi} \log^2 N + O(\alpha_s^2)\right) \tilde{D}_{g \rightarrow Q\bar{Q}({}^3P_J^{[8]})}^{\text{LO}}(N). \quad (15c)$$

We see that not only the threshold double logarithms do appear in quarkonium FFs, they begin to appear at different orders in α_s , because while $D_{g \rightarrow Q\bar{Q}({}^3S_1^{[8]})}$ begins at order α_s , $D_{g \rightarrow Q\bar{Q}({}^3P_J^{[8]})}$ and $D_{g \rightarrow Q\bar{Q}({}^3P_J^{[1]})}$ begin at order α_s^2 . Hence, in a fixed-order calculation, threshold logarithms will be always truncated inconsistently; for example, a fixed-order NLO calculation of quarkonium production rates will include contributions from FFs to order- α_s^2 accuracy, which will include the first threshold double logarithm in the ${}^3S_1^{[8]}$ channel, while the threshold logarithms in the P -wave channels will be neglected. This inconsistency can cause the quarkonium production rates computed at NLO to turn negative at large transverse momentum as the negative correction from the threshold double logarithm in the ${}^3S_1^{[8]}$ gluon FF becomes amplified. Because of this, an all-orders resummation is the only proper way to treat the threshold double logarithms in production of heavy quarkonia.

C. Quark fragmentation and polarized fragmentation functions

Before we move on to the next section, for completeness let us inspect the quark FFs and polarized FFs for production of polarized quarkonia. The results for quark FFs and polarized FFs are summarized in Refs. [34, 39].

Quark FFs appear from order α_s^2 in the ${}^3S_1^{[8]}$ and ${}^3S_1^{[1]}$ channels; they are continuous functions in z , and their Mellin transforms vanish like $1/N$ as $N \rightarrow \infty$. Hence, similarly to the case of the ${}^1S_0^{[8]}$ and ${}^3S_1^{[1]}$ gluon FFs, logarithmic corrections to the quark FF will be power suppressed and will not lead to singular distributions. Due to the quark-gluon mixing in the splitting functions, the threshold logarithms in the ${}^3S_1^{[8]}$ gluon FF may mix into the

quark FF at higher orders in α_s ; however, because the quark-gluon mixing contribution in the splitting function vanishes like $1/N$, these logarithms are always power suppressed when they appear in the quark FF, and do not produce singular distributions in z space.

Finally, let us discuss the singularities in the polarized FFs. It is known from explicit calculations that to order α_s^2 accuracy that the polarized ${}^3S_1^{[8]}$, ${}^1S_0^{[8]}$, and ${}^3P_J^{[8]}$ gluon FFs that produce longitudinally polarized S -wave vector quarkonium are regular functions in z . The same is true for the polarized gluon FFs for the ${}^3S_1^{[1]}$ channel, which begin at order α_s^3 , and also for the quark FFs, which are known through order α_s^2 . Hence, the polarized FFs for production of longitudinally polarized S -wave vector quarkonium do not involve singular distributions in z . In particular, the explicit NLO calculation of polarized ${}^3S_1^{[8]}$ gluon FF shows that the relation in Eq. (15a) for leading threshold double logarithms in the ${}^3S_1^{[8]}$ gluon FF still holds for production of transversely polarized J/ψ or $\psi(2S)$ [17]. In the case of χ_{cJ} or χ_{bJ} production, the helicity decomposition for the ${}^3S_1^{[8]}$ and ${}^3P_J^{[1]}$ FFs shown in Appendix B. indicate that the gluon FF for production of polarized χ_{cJ} or χ_{bJ} contains singularities for every helicity state, and the relation in Eq. (15a) for the ${}^3S_1^{[8]}$ gluon FF holds for every helicity state in the production of polarized χ_{cJ} or χ_{bJ} .

While loop corrections to the ${}^3P_J^{[8]}$ and ${}^3P_J^{[1]}$ gluon FFs have not been computed for the polarized case, we expect that the relation in Eq. (15b) to hold for production of transversely polarized S -wave vector quarkonium, and Eq. (15c) to hold for production of χ_{cJ} or χ_{bJ} for every helicity state, because the attachments of soft gluons that are responsible for generating threshold logarithms do not change the heavy quark spin. We will show this in following sections using the general analysis of threshold logarithms in quarkonium FFs.

III. SOFT FACTORIZATION

In this section, we investigate the $z \rightarrow 1$ behavior of the gluon FFs in the presence of an arbitrary number of soft gluons, which will allow us to compute threshold logarithms to arbitrarily high orders in α_s .

A. Grammer-Yennie approximation

We begin with the operator definition of the gluon FF for production of a hadron H , which is given by [26]

$$D_{g \rightarrow H}(z) = \frac{-g^{\mu\nu} z^{d-3}}{2\pi K^+ (N_c^2 - 1)(d-2)} \int_{-\infty}^{+\infty} dx^- e^{-iK^+ x^-} \times \langle 0 | G_{+\mu}^c(0) \Phi_n^{\dagger bc}(\infty, 0) a_{H(P)}^\dagger a_{H(P)} \Phi_n^{ba}(\infty, x^-) G_{+\nu}^a(nx^-) | 0 \rangle, \quad (16)$$

where K is the momentum of the initial-state gluon, $G_{\mu\nu} = G_{\mu\nu}^a T^a$ is the QCD field-strength tensor, $\Phi_k^{ab}(y, x)$ is a path-ordered exponential of the gluon field in the k direction in the adjoint representation defined by

$$\Phi_k(y, x) = \mathcal{P} \exp \left[-ig \int_x^y d\lambda k \cdot A^{\text{adj}}(k\lambda) \right], \quad (17)$$

with \mathcal{P} the path ordering, n is a lightlike vector defined through $n \cdot K = K^+$, and $a_{H(P)}$ is an operator that annihilates a H with momentum P , so that $a_{H(P)}^\dagger a_{H(P)}$ projects onto states that contain a H with momentum P . Our goal is to find the $z \rightarrow 1$ behavior for production of a $Q\bar{Q}$ in a specific color and angular momentum state. The production of a $Q\bar{Q}$ from a fragmenting gluon occurs through the process $g^* \rightarrow Q\bar{Q}$, followed by radiation of an arbitrary number of gluons from Q and \bar{Q} lines. Because we are interested in the region $z \approx 1$, we only consider the case where the gluon attachments to Q or \bar{Q} are soft. In this case, we can apply the Grammer-Yennie approximation (soft approximation) to simplify the Feynman rule for soft-gluon vertices [25, 27, 40]. The outermost gluon attachment to the Q line can be simplified as

$$\begin{aligned} \bar{u}(p_1) \gamma^\mu T^a \frac{i(p_1 + \not{k} + m)}{(p_1 + k)^2 - m^2 + i\varepsilon} &= \bar{u}(p_1) T^a \frac{i[2(p_1^\mu + k^\mu) - (p_1 + \not{k})\gamma^\mu + m\gamma^\mu]}{2p_1 \cdot k + k^2 + i\varepsilon} \\ &= \bar{u}(p_1) T^a \frac{i[2(p_1^\mu + k^\mu) - \not{k}\gamma^\mu]}{2p_1 \cdot k + k^2 + i\varepsilon} \\ &\approx \bar{u}(p_1) T^a \frac{ip_1^\mu}{p_1 \cdot k + i\varepsilon}, \end{aligned} \quad (18)$$

where p_1 is the momentum of the Q , and k is the outgoing momentum of the gluon. In the last line, we neglected k compared to p_1 in the numerator, and neglected k^2 compared to $p_1 \cdot k$ in the denominator. Similarly, the outermost gluon attachment to the \bar{Q} line can be

simplified as

$$\begin{aligned}
\frac{i(-\not{p}_2 - \not{k} + m)}{(p_2 + k)^2 - m^2 + i\varepsilon} \gamma^\mu T^a v(p_2) &= \frac{i[-2(p_2^\mu + k^\mu) + \gamma^\mu(\not{p}_2 + \not{k}) + m\gamma^\mu]}{2p_2 \cdot k + k^2 + i\varepsilon} T^a v(p_2) \\
&= -\frac{i[2(p_2^\mu + k^\mu) - \gamma^\mu \not{k}]}{2p_2 \cdot k + k^2 + i\varepsilon} T^a v(p_2) \\
&\approx -\frac{ip_2^\mu}{p_2 \cdot k + i\varepsilon} T^a v(p_2),
\end{aligned} \tag{19}$$

with p_2 the momentum of the \bar{Q} . For multiple gluon attachments, the same approximation can be applied sequentially, beginning with the outermost gluon attachment. An n -gluon attachment to a Q line in the soft approximation leads to

$$\bar{u}(p_1) \frac{ip_1^{\mu_1} T^{a_1}}{p_1 \cdot k_1 + i\varepsilon} \frac{ip_1^{\mu_2} T^{a_2}}{p_1 \cdot k_2 + i\varepsilon} \dots \frac{ip_1^{\mu_n} T^{a_n}}{p_1 \cdot k_n + i\varepsilon}, \tag{20}$$

where μ_i and a_i are the Lorentz and color indices of the i th gluon, respectively, and k_i is the momentum carried by the i th gluon. This is equivalent to the Feynman rule for n -gluon attachment to the path ordered, time ordered Wilson line in the p_1 direction, defined by

$$W_{p_1}(t', t) = \mathcal{P} \exp \left[-ig \int_t^{t'} d\lambda p_1 \cdot A(p_1 \lambda) \right]. \tag{21}$$

Similarly, soft-gluon attachments to the \bar{Q} line is equivalent to the anti-path ordered, time ordered Wilson line in the p_2 direction:

$$W_{p_2}^\dagger(t', t) = \bar{\mathcal{P}} \exp \left[+ig \int_t^{t'} d\lambda p_2 \cdot A(p_2 \lambda) \right], \tag{22}$$

with $\bar{\mathcal{P}}$ the anti-path ordering. This lets us write the amplitude for $g^* \rightarrow Q\bar{Q}$ followed by radiation of an arbitrary number of soft gluons as the operator

$$\mathcal{A}_{\text{soft}}^{\mu, a} = T \left[\bar{u}(p_1) W_{p_1}(\infty, 0) (-ig\gamma^\mu T^a) W_{p_2}^\dagger(\infty, 0) v(p_2) \right], \tag{23}$$

where T is the time ordering, and μ and a are the Lorentz and color indices of the fragmenting gluon, respectively. Then the gluon fragmentation function in the soft approximation can be written as

$$\begin{aligned}
D_{g \rightarrow Q\bar{Q}}^{\text{soft}}(z) &= 2M(-g^{\mu\nu}) C_{\text{frag}} \left| \frac{-i}{K^2 + i\varepsilon} \right|^2 \left(g_{\mu\alpha} - \frac{K_\mu n_\alpha}{K^+} \right) \left(g_{\nu\beta} - \frac{K_\nu n_\beta}{K^+} \right) \\
&\times \langle 0 | \bar{T} \left[\mathcal{A}_{\text{soft}}^{\beta, c} \Phi_n^{bc}(\infty, 0) \right]^\dagger 2\pi\delta(n \cdot \hat{p} - P^+(1-z)) T \left[\mathcal{A}_{\text{soft}}^{\alpha, a} \Phi_n^{ba}(\infty, 0) \right] | 0 \rangle,
\end{aligned} \tag{24}$$

where $M = \sqrt{P^2}$, $C_{\text{frag}} = z^{d-3}K^+/[2\pi(N_c^2 - 1)(d - 2)]$, \bar{T} is antitime ordering, and \hat{p} is the operator that reads off the momentum of the operator to the right. The $-i/(K^2 + i\varepsilon)$ is the propagator of the fragmenting gluon, and tensors $g_{\mu\alpha} - K_\mu n_\alpha/K^+$ and $g_{\nu\beta} - K_\nu n_\beta/K^+$ arise from the Feynman rule of the operators $G_{+\mu}^c$ and $G_{+\nu}^a$ that create and annihilate the gluon in the definition of the gluon FF. The delta function arises from the Fourier transform in Eq. (16).

Eq. (24) can be considered a soft factorization formula, where the $z \approx 1$ behavior of the FF is contained in the soft function, which is given by the vacuum expectation value. Hence, we can investigate the singularities in the gluon FF at $z = 1$ by computing the soft function, rather than the gluon FF itself. Note that while the matching coefficient of this soft factorization formula can also receive radiative corrections, our determination at leading nonvanishing order in α_s is sufficient for computing the leading threshold logarithms, which is the goal of this work. Note that, because now the singularities in z are completely included in the soft function, any residual z dependence in the coefficient can be neglected by setting $K = P$ in Eq. (24). We can already calculate the tensors in Eq. (24) as

$$(-g_{\mu\nu}) \left(g^{\mu\alpha} - \frac{P^\mu n^\alpha}{P^+} \right) \left(g^{\nu\beta} - \frac{P^\nu n^\beta}{P^+} \right) = -g^{\alpha\beta} + \frac{P^\alpha n^\beta + P^\beta n^\alpha}{P^+} - \frac{P^2 n^\alpha n^\beta}{(P^+)^2} \equiv I_T^{\alpha\beta}, \quad (25)$$

which satisfies $I_T^{\alpha\beta} = I_T^{\beta\alpha}$ and $I_T^{\alpha\beta} P_\alpha = I_T^{\alpha\beta} n_\alpha = 0$. The tensor $I_T^{\alpha\beta}$ can be identified as the transverse polarization sum for a spin-1 boson with momentum P [41]. Hence,

$$D_{g \rightarrow Q\bar{Q}}^{\text{soft}}(z) = 2MC_{\text{frag}} \left| \frac{-i}{K^2 + i\varepsilon} \right|^2 I_T^{\alpha\beta} S_{\alpha\beta}(z), \quad (26)$$

where $S_{\alpha\beta}(z)$ is the soft function defined by

$$S^{\alpha\beta}(z) \equiv \langle 0 | \bar{T} \left[\mathcal{A}_{\text{soft}}^{\beta,c} \Phi_n^{bc}(\infty, 0) \right]^\dagger 2\pi\delta(n \cdot \hat{p} - P^+(1 - z)) T \left[\mathcal{A}_{\text{soft}}^{\alpha,a} \Phi_n^{ba}(\infty, 0) \right] | 0 \rangle, \quad (27)$$

While it is in principle possible to tackle the soft function $S^{\alpha\beta}(z)$ directly, the calculation can be further simplified by projecting the final-state $Q\bar{Q}$ onto specific color and angular momentum states, which will also allow a more direct comparison with fixed-order results for the FFs.

B. Spin and color projectors

We use the projector method to project the Dirac spinors in the soft amplitude $\mathcal{A}_{\text{soft}}^{\mu,a}$ onto specific color and angular momentum. We take the nonrelativistic normalization for

the spinors, and take the conventions used in Ref. [42]. In the spin-triplet case, this is done by the replacement

$$\bar{u}(p_1)\Gamma v(p_2) \rightarrow \frac{N_1 N_2}{2\sqrt{2}M} \text{tr} [(\not{p}_2 - m)\not{\epsilon}_S^*(\not{P} + M)(\not{p}_1 + m)\Lambda_c \Gamma], \quad (28)$$

where the trace is over Dirac and color matrices, $\Gamma = W_{p_1}(\infty, 0)(-ig\gamma^\mu T^a)W_{p_2}^\dagger(\infty, 0)$, $p_1^2 = p_2^2 = m^2$, $P^2 = M^2$, $N_i = 1/\sqrt{2E_i(E_i + m)}$ with $E_i = p_i \cdot P/M$, ϵ_S is the polarization vector for the $Q\bar{Q}$ spin in the spin-triplet state, and Λ_c is the color projector for color-singlet ($c = 1$) and octet ($c = 8$) states given by

$$\Lambda_1 = \frac{\mathbf{1}}{\sqrt{N_c}}, \quad (29)$$

$$\Lambda_8^a = \frac{T^a}{\sqrt{T_F}}, \quad (30)$$

with $\mathbf{1}$ the $SU(N_c)$ unit matrix. The projection onto specific orbital angular momentum states is done by expressing the soft amplitude as a function of $p = (p_1 + p_2)/2 = P/2$ and the relative momentum $q = (p_1 - p_2)/2$, and then expanding in powers of q . The S -wave contribution is the $q = 0$ term, and the P -wave contribution comes from the term linear in q . As the only Dirac matrix in Γ is γ^μ , the only Dirac trace that we need is

$$\frac{N_1 N_2}{2\sqrt{2}M} \text{tr}_{\text{Dirac}} [(\not{p}_2 - m)\not{\epsilon}_S^*(\not{P} + M)(\not{p}_1 + m)\gamma^\mu] = -\sqrt{2}\epsilon_S^{*\mu} - \frac{4\sqrt{2}q^\mu \epsilon_S^* \cdot q}{M(M + 2m)}, \quad (31)$$

where we used $p \cdot \epsilon_S^* = 0$. The right-hand side is equivalent to Eq. (A9b) of Ref. [30] up to a phase and normalization convention. Note that since $M = 2\sqrt{m^2 - q^2}$, the right-hand side does not involve terms linear in q when expanded in powers of q , as the second term on the right-hand side is already quadratic in q . Since we are only interested in the S - and P -wave states, we only need to retain the first term on the right-hand side in our calculation of the soft function. The color trace in the soft amplitude is given by

$$\text{tr}_{\text{color}} [\Lambda_c W_{p_1}(\infty, 0)T^a W_{p_2}^\dagger(\infty, 0)], \quad (32)$$

which is in general a function of p and q . When expanded in powers of q , this can be expressed in terms of the adjoint Wilson line and the field-strength tensor by using Polyakov's identity [43]. We carry out this calculation for each color and angular momentum state.

C. ${}^3S_1^{[8]}$

In order to project onto the S -wave state, we expand the soft amplitude in powers of the relative momentum q and retain only the $q = 0$ contribution. As the Dirac trace is already computed in the previous section, we only need to consider the color trace, which we compute at $q = 0$. We make use of the following identities for products of Wilson lines

$$W_p(\lambda_f, \lambda_i) = W_p(\lambda_f, \lambda)W_p(\lambda, \lambda_i), \quad (33a)$$

$$W_p(\lambda_f, \lambda_i)T^aW_p^\dagger(\lambda_f, \lambda_i) = T^b\Phi_p^{ba}(\lambda_f, \lambda_i), \quad (33b)$$

$$W_p^\dagger(\lambda_f, \lambda_i)T^aW_p(\lambda_f, \lambda_i) = \Phi_p^{ab}(\lambda_f, \lambda_i)T^b, \quad (33c)$$

$$W_p(\lambda_f, \lambda_i)W_p^\dagger(\lambda_f, \lambda_i) = 1, \quad (33d)$$

which hold for $\lambda_f > \lambda > \lambda_i$. From these we obtain

$$\begin{aligned} \frac{1}{\sqrt{T_F}}\text{tr}_{\text{color}}(W_p(\infty, 0)T^aW_p^\dagger(\infty, 0)T^d) &= \frac{1}{\sqrt{T_F}}\Phi_p^{ba}(\infty, 0)\text{tr}_{\text{color}}(T^bT^d) \\ &= \sqrt{T_F}\Phi_p^{da}(\infty, 0), \end{aligned} \quad (34)$$

where d is the adjoint color index for the ${}^3S_1^{[8]}$ state. By combining this with the result for the Dirac trace we obtain

$$\mathcal{A}_{\text{soft}}^{\mu, a; d}({}^3S_1^{[8]}) = \sqrt{2T_F}ig\epsilon_S^{*\mu}\Phi_p^{da}(\infty, 0). \quad (35)$$

By plugging this to Eq. (24) we obtain

$$D_{g \rightarrow Q\bar{Q}({}^3S_1^{[8]})}^{\text{soft}}(z) = 2M \left| \frac{-i}{P^2} \right|^2 C_{\text{frag}} 2T_F g^2 I_T^{\alpha\beta} \sum_{\lambda} \epsilon_{S\alpha}^*(\lambda) \epsilon_{S\beta}(\lambda) S_{{}^3S_1^{[8]}}(z), \quad (36)$$

where we define the ${}^3S_1^{[8]}$ soft function as

$$S_{{}^3S_1^{[8]}}(z) \equiv \langle 0 | [\mathcal{W}({}^3S_1^{[8]})^{cb}]^\dagger 2\pi\delta(n \cdot \hat{p} - P^+(1-z)) \mathcal{W}({}^3S_1^{[8]})^{cb} | 0 \rangle, \quad (37)$$

with

$$\mathcal{W}({}^3S_1^{[8]})^{cb} \equiv T \left[\Phi_p^{ca}(\infty, 0) \Phi_n^{ba}(\infty, 0) \right]. \quad (38)$$

The polarization sum is evaluated by using

$$\sum_{\lambda} \epsilon_{S\alpha}^*(\lambda) \epsilon_{S\beta}(\lambda) = I_{\alpha\beta} \equiv -g_{\alpha\beta} + \frac{P_{\alpha}P_{\beta}}{P^2}, \quad (39)$$

which yields

$$D_{g \rightarrow Q\bar{Q}(^3S_1^{[8]})}^{\text{soft}}(z) = \frac{C_{\text{frag}}(d-2)g^2}{4m^3} S_{^3S_1^{[8]}}(z). \quad (40)$$

We note that, because the tensor $I_T^{\alpha\beta}$ vanishes when contracted with a longitudinal polarization vector, there is no contribution to $D_{g \rightarrow Q\bar{Q}(^3S_1^{[8]})}^{\text{soft}}$ coming from longitudinally polarized $Q\bar{Q}$ in the $^3S_1^{[8]}$ state.

D. $^3P^{[8]}$

We next consider the $^3P^{[8]}$ case. As we have discussed previously, the Dirac trace does not involve terms linear in q , so that we can set $q = 0$ in Eq. (31). Hence, the only term linear in q can come from the expansion of the color trace in powers of q . The expansion can be carried out by using a straightforward generalization of Polyakov's identity [27, 43] :

$$\begin{aligned} \delta \mathcal{P} \exp \left[-ig \oint_C d\lambda A_\alpha(x(\lambda)) \frac{dx^\alpha(\lambda)}{d\lambda} \right] &= \mathcal{P} \oint_C ds \exp \left[-ig \int_s^{\lambda_f} d\lambda A_\alpha(x(\lambda)) \frac{dx^\alpha(\lambda)}{d\lambda} \right] \\ &\times (-ig) G_{\mu\nu}(x(s)) \frac{dx^\nu(s)}{ds} \exp \left[-ig \int_{\lambda_i}^s d\lambda' A_\alpha(x(\lambda')) \frac{dx^\alpha(\lambda')}{d\lambda'} \right] \delta x^\mu(s), \end{aligned} \quad (41)$$

where C is a closed path in spacetime parametrized by $x(\lambda)$, δx is the variation of the path, and $x(\lambda_i) = x(\lambda_f)$ is an arbitrary point on C . We use this identity to expand the $W_{p_1}(\infty, 0)$ and $W_{p_2}^\dagger(\infty, 0)$ in the color trace to linear power in q . We obtain

$$\begin{aligned} W_{p_1}(\infty, 0) T^a W_{p_2}^\dagger(\infty, 0) &= \left[W_p(\infty, 0) - ig \int_0^\infty d\lambda \lambda W_p(\infty, \lambda) G_{\mu\nu}(p\lambda) p^\mu q^\nu W_p(\lambda, 0) + O(q^2/p^2) \right] T^a W_{p_2}^\dagger(\infty, 0) \\ &= \left[W_p(\infty, 0) T^a W_p^\dagger(\infty, 0) - ig \int_0^\infty d\lambda \lambda W_p(\infty, \lambda) G_{\mu\nu}(p\lambda) p^\mu q^\nu W_p(\lambda, 0) T^a W_p^\dagger(\infty, 0) \right. \\ &\quad \left. + ig \int_0^\infty d\lambda \lambda W_p(\infty, 0) T^a W_p^\dagger(\lambda, 0) G_{\mu\nu}(p\lambda) p^\mu (-q^\nu) W_p^\dagger(\infty, \lambda) + O(q^2/p^2) \right]. \end{aligned} \quad (42)$$

The first term in the square brackets is the $q = 0$ term, and the remaining terms are linear in q . The P -wave contribution corresponds to the coefficient of q in the linear term. We take the normalization used in Ref. [33], where the P -wave contribution in the linear term $A_\alpha q^\alpha$ in the amplitude is given by $A_\alpha \epsilon_L^\alpha / \sqrt{d-1}$, with ϵ_L the polarization vector for the orbital angular momentum of the $Q\bar{Q}$. In this normalization, the color-octet P -wave contribution

of the color trace is given by

$$\begin{aligned} & \text{tr}_{\text{color}} \left[W_{p_1}(\infty, 0) T^a W_{p_2}^\dagger(\infty, 0) \Lambda_8^{a'} \right]_{P-\text{wave}} \\ &= \frac{ig\epsilon_L^{*\nu}}{\sqrt{T_F(d-1)}} \int_0^\infty d\lambda \lambda \text{tr}_{\text{color}} \left[W_p^\dagger(\infty, 0) T^{a'} W_p(\infty, \lambda) p^\mu G_{\mu\nu}^b(p\lambda) T^b W_p(\lambda, 0) T^a \right. \\ & \quad \left. + T^a W_p^\dagger(\lambda, 0) p^\mu G_{\mu\nu}^b(p\lambda) T^b W_p^\dagger(\infty, \lambda) T^{a'} W_p(\infty, 0) \right]. \end{aligned} \quad (43)$$

We can now use the identities in Eqs. (33) and the cyclic property of the trace to reduce the fundamental Wilson lines into adjoint ones. We have

$$\text{tr}_{\text{color}}[W_p^\dagger(\infty, 0) T^{a'} W_p(\infty, \lambda) T^b W_p(\lambda, 0) T^a] = \text{tr}_{\text{color}}[\Phi^{a'c}(\infty, \lambda) T^c T^b T^d \Phi_p^{da}(\lambda, 0)], \quad (44)$$

$$\text{tr}_{\text{color}}[T^a W_p^\dagger(\lambda, 0) T^b W_p^\dagger(\infty, \lambda) T^{a'} W_p(\infty, 0)] = \text{tr}_{\text{color}}[\Phi_p^{da}(\lambda, 0) T^d T^b \Phi_p^{a'c}(\infty, \lambda) T^c], \quad (45)$$

which lead to

$$\begin{aligned} & \text{tr}_{\text{color}} \left[W_{p_1}(\infty, 0) T^a W_{p_2}^\dagger(\infty, 0) \Lambda_8^{a'} \right]_{P-\text{wave}} \\ &= \frac{ig\epsilon_L^{*\nu}}{\sqrt{2(d-1)}} \int_0^\infty d\lambda \lambda \Phi_p^{a'c}(\infty, \lambda) d^{bcd} p^\mu G_{\mu\nu}^b(p\lambda) \Phi_p^{da}(\lambda, 0), \end{aligned} \quad (46)$$

where we used $\text{tr}_{\text{color}}(\{T^b, T^c\} T^d) = T_F d^{bcd}$ and $T_F = 1/2$. Note that $d^{bcd} p^\mu G_{\mu\nu}^b(p\lambda)$ is a rank-2 tensor in the adjoint representation of $SU(N_c)$, and is a Lorentz vector that is orthogonal to p^ν . By using this result we obtain the fragmentation function in the soft approximation

$$\begin{aligned} D_{g \rightarrow Q\bar{Q}(^3P^{[8]})}^{\text{soft}}(z) &= \frac{1}{4m^3} \frac{g^2}{2(d-1)} 2g^2 C_{\text{frag}} I_T^{\alpha\alpha'} \sum_{\lambda_S} \epsilon_{S\alpha}^*(\lambda_S) \epsilon_{S\alpha'}(\lambda_S) \sum_{\lambda_L} \epsilon_L^{*\beta}(\lambda_L) \epsilon_L^{\beta'}(\lambda_L) \\ & \times \langle 0 | [\mathcal{W}_{\beta'}^{yx}(^3P^{[8]})]^\dagger 2\pi\delta(n \cdot \hat{p} - P^+(1-z)) \mathcal{W}_\beta^{yx}(^3P^{[8]}) | 0 \rangle, \end{aligned} \quad (47)$$

where

$$\mathcal{W}_\beta^{yx}(^3P^{[8]}) \equiv T \left[\int_0^\infty d\lambda \lambda \Phi_p^{yc}(\infty, \lambda) p^\mu G_{\mu\beta}^b(p\lambda) d^{bcd} \Phi_p^{da}(\lambda, 0) \Phi_n^{xa}(\infty, 0) \right]. \quad (48)$$

The polarization sums are given by

$$\sum_{\lambda_S} \epsilon_S^{*\alpha}(\lambda_S) \epsilon_S^{\alpha'}(\lambda_S) = \sum_{\lambda_L} \epsilon_L^{*\alpha}(\lambda_L) \epsilon_L^{\alpha'}(\lambda_L) = I^{\alpha\alpha'} = -g^{\alpha\alpha'} + \frac{P^\alpha P^{\alpha'}}{P^2}. \quad (49)$$

Since $\mathcal{W}_\beta^{yx}(^3P^{[8]})$ is orthogonal to p^β , we may neglect the $P^\beta P^{\beta'}/P^2$ term in the polarization sum of $\epsilon_L^{*\beta}(\lambda_L) \epsilon_L^{\beta'}(\lambda_L)$. From this we obtain

$$D_{g \rightarrow Q\bar{Q}(^3P^{[8]})}^{\text{soft}}(z) = -\frac{1}{4m^3} \frac{g^4(d-2)}{(d-1)} C_{\text{frag}} S_{^3P^{[8]}}(z), \quad (50)$$

where $S_{3P[8]}(z)$ is the ${}^3P^{[8]}$ soft function defined by

$$S_{3P[8]}(z) \equiv \langle 0 | [\mathcal{W}_{\beta'}^{yx}({}^3P^{[8]})]^\dagger 2\pi\delta(n \cdot \hat{p} - P^+(1-z)) \mathcal{W}_\beta^{yx}({}^3P^{[8]}) | 0 \rangle g^{\beta\beta'}. \quad (51)$$

Similarly to the ${}^3S_1^{[8]}$ case, the contribution from longitudinal $Q\bar{Q}$ spin vanishes because $\epsilon_{S\alpha}^*(\lambda_S)$ is contracted with the tensor $I_T^{\alpha\alpha'}$.

E. ${}^3P_J^{[1]}$

Finally, we consider the ${}^3P_J^{[1]}$ state. The calculation is similar to the ${}^3P^{[8]}$ state, except that we project onto the color-singlet state. We have

$$\begin{aligned} & \text{tr}_{\text{color}} [W_{p1}(\infty, 0) T^a W_{p2}^\dagger(\infty, 0) \Lambda_1]_{P-\text{wave}} \\ &= \frac{ig\epsilon_L^{*\nu}}{\sqrt{N_c(d-1)}} \int_0^\infty d\lambda' \lambda' \text{tr}_{\text{color}} \left[W_p^\dagger(\infty, 0) W_p(\infty, \lambda') p^\mu G_{\mu\nu}^b(p\lambda') T^b W_p(\lambda', 0) T^a \right. \\ & \quad \left. + T^a W_p^\dagger(\lambda', 0) p^\mu G_{\mu\nu}^b(p\lambda') T^b W_p^\dagger(\infty, \lambda') W_p(\infty, 0) \right], \end{aligned} \quad (52)$$

where again ϵ_L is the polarization vector for the orbital angular momentum of the $Q\bar{Q}$. By using the identities in Eqs. (33) we obtain

$$\begin{aligned} & \text{tr}_{\text{color}} [W_{p1}(\infty, 0) T^a W_{p2}^\dagger(\infty, 0) \Lambda_1]_{P-\text{wave}} \\ &= \frac{2T_F\epsilon_L^{*\nu}}{\sqrt{N_c(d-1)}} ig \int_0^\infty d\lambda' \lambda' p^\mu G_{\mu\nu}^b(p\lambda') \Phi_p^{ba}(\lambda', 0). \end{aligned} \quad (53)$$

From this we obtain

$$D_{g \rightarrow Q\bar{Q}({}^3P^{[1]})}^{\text{soft}}(z) = \frac{1}{4m^3} \frac{2g^4}{N_c(d-1)} C_{\text{frag}} I_T^{\alpha\alpha'} \epsilon_{S\alpha}^* \epsilon_{S\alpha'} \epsilon_{L\beta}^* \epsilon_{L\beta'} S_{3P^{[1]}}^{\beta\beta'}(z), \quad (54)$$

where

$$S_{3P^{[1]}}^{\beta\beta'} \equiv \langle 0 | [\mathcal{W}^{\beta\beta'}({}^3P^{[1]})]^\dagger 2\pi\delta(n \cdot \hat{p} - P^+(1-z)) \mathcal{W}^{b\beta}({}^3P^{[1]}) | 0 \rangle, \quad (55)$$

$$\mathcal{W}_\beta^b({}^3P^{[1]}) \equiv \int_0^\infty d\lambda \lambda p^\mu G_{\mu\beta}^d(p\lambda) \Phi_p^{da}(\lambda, 0) \Phi_n^{ba}(\infty, 0). \quad (56)$$

For the ${}^3P_J^{[1]}$ channel, the polarization sums need to be done for specific $J = 0, 1$, and 2 . This can be done by making the replacements $\epsilon_{S\alpha}^* \epsilon_{S\alpha'} \epsilon_{L\beta}^* \epsilon_{L\beta'} \rightarrow \Pi_{\alpha\beta\alpha'\beta'}^J$, where

$$\begin{aligned} \Pi_{\alpha\beta\alpha'\beta'}^{J=0} &= \frac{1}{d-1} I_{\alpha\beta} I_{\alpha'\beta'}, \\ \Pi_{\alpha\beta\alpha'\beta'}^{J=1} &= \frac{1}{2} (I_{\alpha\alpha'} I_{\beta\beta'} - I_{\alpha\beta'} I_{\alpha'\beta}) \\ \Pi_{\alpha\beta\alpha'\beta'}^{J=2} &= \frac{1}{2} (I_{\alpha\alpha'} I_{\beta\beta'} + I_{\alpha\beta'} I_{\alpha'\beta}) - \frac{1}{d-1} I_{\alpha\beta} I_{\alpha'\beta'}. \end{aligned} \quad (57)$$

Note that $\sum_J \Pi_{\alpha\beta\alpha'\beta'}^J = I_{\alpha\alpha'} I_{\beta\beta'}$. This gives

$$I_T^{\alpha\alpha'} \Pi_{\alpha\beta\alpha'\beta'}^J S_{3P^{[1]}}^{\beta\beta'} = S_{3P^{[1]}}^{\beta\beta'} \times \begin{cases} -\frac{1}{d-1} \left(g_{\beta\beta'} + \frac{P^2 n_\beta n_{\beta'}}{P_+^2} \right) & (J=0) \\ -\frac{d-3}{2} g_{\beta\beta'} + \frac{1}{2} \frac{P^2 n_\beta n_{\beta'}}{P_+^2} & (J=1) \\ -\frac{d^2-2d-1}{2(d-1)} g_{\beta\beta'} - \frac{d-3}{2(d-1)} \frac{P^2 n_\beta n_{\beta'}}{P_+^2} & (J=2) \end{cases} \quad (58)$$

Here, we eliminated the terms involving P^β and $P^{\beta'}$ in $\Pi_{\alpha\beta\alpha'\beta'}^J$ by using $S_{3P^{[1]}}^{\beta\beta'} P_\beta = S_{3P^{[1]}}^{\beta'\beta} P_\beta = 0$. The $n_\beta n_{\beta'}$ terms can be rewritten as

$$n_\beta n_{\beta'} = -\frac{(n \cdot p)^2}{p^2(d-1)} g_{\beta\beta'} + \left(n_\beta n_{\beta'} + \frac{(n \cdot p)^2}{p^2(d-1)} g_{\beta\beta'} \right), \quad (59)$$

where the terms in the parenthesis vanishes when contracted with the isotropic tensor $I^{\beta\beta'}$.

By using this we can write the isotropic and anisotropic contributions as

$$I_T^{\alpha\alpha'} \Pi_{\alpha\beta\alpha'\beta'}^J S_{3P^{[1]}}^{\beta\beta'} \Big|_{\text{isotropic}} = -(d-2) S_{3P^{[1]}}^{\beta\beta'} g_{\beta\beta'} \times \begin{cases} \frac{1}{(d-1)^2} & (J=0) \\ \frac{(d-2)}{2(d-1)} & (J=1) \\ \frac{(d-2)(d+1)}{2(d-1)^2} & (J=2) \end{cases} \quad (60)$$

and

$$I_T^{\alpha\alpha'} \Pi_{\alpha\beta\alpha'\beta'}^J S_{3P^{[1]}}^{\beta\beta'} \Big|_{\text{anisotropic}} = S_{3P^{[1]}}^{\beta\beta'} \left(\frac{p^2 n_\beta n_{\beta'}}{p_+^2} + \frac{g_{\beta\beta'}}{d-1} \right) \times \begin{cases} -\frac{1}{d-1} & (J=0) \\ \frac{1}{2} & (J=1) \\ -\frac{d-3}{2(d-1)} & (J=2) \end{cases} \quad (61)$$

From these we can write

$$D_{g \rightarrow Q\bar{Q}(^3P_J^{[1]})}^{\text{soft}}(z) = -\frac{1}{4m^3} \frac{2(d-2)g^4}{N_c(d-1)} C_{\text{frag}} \left[c^J S_{3P^{[1]}}(z) + c_{TT}^J S_{3P^{[1]}}^{TT}(z) \right], \quad (62)$$

where

$$S_{3P^{[1]}}(z) = \langle 0 | [\mathcal{W}_{\beta'}^b(^3P^{[1]})]^\dagger 2\pi \delta(n \cdot \hat{p} - P^+(1-z)) \mathcal{W}_\beta^b(^3P^{[1]}) | 0 \rangle g^{\beta\beta'}, \quad (63a)$$

$$S_{3P^{[1]}}^{TT}(z) = \langle 0 | [\mathcal{W}_{\beta'}^b(^3P^{[1]})]^\dagger 2\pi \delta(n \cdot \hat{p} - P^+(1-z)) \mathcal{W}_\beta^b(^3P^{[1]}) | 0 \rangle \left(\frac{p^2 n^\beta n^{\beta'}}{p_+^2} + \frac{g^{\beta\beta'}}{d-1} \right), \quad (63b)$$

with

$$c^J = \begin{cases} \frac{1}{(d-1)^2} & (J=0) \\ \frac{(d-2)}{2(d-1)} & (J=1) \\ \frac{(d-2)(d+1)}{2(d-1)^2} & (J=2) \end{cases}, \quad (64a)$$

$$-(d-2) \times c_{TT}^J = \begin{cases} -\frac{1}{d-1} & (J=0) \\ \frac{1}{2} & (J=1) \\ -\frac{d-3}{2(d-1)} & (J=2) \end{cases}. \quad (64b)$$

Note that $\sum_{J=0}^2 c^J = 1$, $c^J = (2J+1)/9 + O(\epsilon)$, and $\sum_{J=0}^2 c_{TT}^J = 0$.

We also consider the polarized case. The polarized spin sums are computed by using [39]

$$\Pi_{\alpha\beta\alpha'\beta'}^{J=1,|h|=1} = \frac{1}{2} (I_{T\alpha\alpha'} I_{L\beta\beta'} + I_{L\alpha\alpha'} I_{T\beta\beta'} - I_{T\alpha\beta'} I_{L\alpha'\beta} - I_{L\alpha\beta'} I_{T\alpha'\beta}), \quad (65)$$

$$\Pi_{\alpha\beta\alpha'\beta'}^{J=1,h=0} = \frac{1}{2} (I_{T\alpha\alpha'} I_{T\beta\beta'} - I_{T\alpha\beta'} I_{T\alpha'\beta}), \quad (66)$$

$$\Pi_{\alpha\beta\alpha'\beta'}^{J=2,|h|=2} = \frac{1}{2} (I_{T\alpha\alpha'} I_{T\beta\beta'} + I_{T\alpha\beta'} I_{T\alpha'\beta}) - \frac{1}{2} I_{T\alpha\beta} I_{T\alpha'\beta'}, \quad (67)$$

$$\Pi_{\alpha\beta\alpha'\beta'}^{J=2,|h|=1} = \frac{1}{2} (I_{T\alpha\alpha'} I_{L\beta\beta'} + I_{L\alpha\alpha'} I_{T\beta\beta'} + I_{T\alpha\beta'} I_{L\alpha'\beta} + I_{L\alpha\beta'} I_{T\alpha'\beta}), \quad (68)$$

$$\Pi_{\alpha\beta\alpha'\beta'}^{J=2,h=0} = \frac{d-2}{d-1} \left(I_{L\alpha\beta} - \frac{1}{d-2} I_{T\alpha\beta} \right) \left(I_{L\alpha'\beta'} - \frac{1}{d-2} I_{T\alpha'\beta'} \right), \quad (69)$$

where $\Pi_{\alpha\beta\alpha'\beta'}^{J,|h|=1} = \sum_{h=\pm 1} \Pi_{\alpha\beta\alpha'\beta'}^{J,h}$, $\Pi_{\alpha\beta\alpha'\beta'}^{J,|h|=2} = \sum_{h=\pm 2} \Pi_{\alpha\beta\alpha'\beta'}^{J,h}$, and $I_L^{\alpha\beta} = I^{\alpha\beta} - I_T^{\alpha\beta}$. We have

$$D_{g \rightarrow Q\bar{Q}(^3P_{J,h}^{[1]})}^{\text{soft}} = -\frac{1}{4m^3} \frac{2(d-2)g^4}{N_c(d-1)} C_{\text{frag}} \left[c^{J,h} S_{^3P^{[1]}}(z) + c_{TT}^{J,h} S_{^3P^{[1]}}^{TT}(z) \right], \quad (70)$$

where

$$c^{J=1,|h|=1} = \frac{1}{2(d-1)}, \quad (71a)$$

$$c^{J=1,h=0} = \frac{(d-3)}{2(d-1)}, \quad (71b)$$

$$c^{J=2,|h|=2} = \frac{d(d-3)}{2(d-1)(d-2)}, \quad (71c)$$

$$c^{J=2,|h|=1} = \frac{1}{2(d-1)}, \quad (71d)$$

$$c^{J=2,h=0} = \frac{1}{(d-1)^2(d-2)}, \quad (71e)$$

$$-(d-2) \times c_{TT}^{J=1,|h|=1} = \frac{d-2}{2}, \quad (71f)$$

$$-(d-2) \times c_{TT}^{J=1,h=0} = -\frac{d-3}{2}, \quad (71g)$$

$$-(d-2) \times c_{TT}^{J=2,|h|=2} = -\frac{d(d-3)}{2(d-2)}, \quad (71h)$$

$$-(d-2) \times c_{TT}^{J=2,|h|=1} = \frac{d-2}{2}, \quad (71i)$$

$$-(d-2) \times c_{TT}^{J=2,h=0} = -\frac{1}{(d-1)(d-2)}. \quad (71j)$$

F. Summary of soft factorization

We now summarize the results of the soft factorization in this section. The general soft factorization formula in Eq. (26) is obtained by applying the Grammer-Yennie approximation (soft approximation) to gluon attachments to the Q and \bar{Q} lines in the process $g^* \rightarrow Q\bar{Q}$. The soft function we obtain is given in Eq. (27), which is valid for $Q\bar{Q}$ in an arbitrary color and angular momentum state. While it is in principle possible to tackle the general soft function in Eq. (27) directly, as was done in Ref. [44], the calculation can be further simplified by projecting the final-state $Q\bar{Q}$ onto specific color and angular momentum states. The resulting soft factorization formulas are given in Eqs. (40), (50), and (62) for the $^3S_1^{[8]}$, $^3P^{[8]}$, and $^3P_J^{[1]}$ states, respectively, with the corresponding soft functions given in Eqs. (37), (51), and (63). These soft functions for specific color and angular momentum states are given by vacuum expectation values of adjoint Wilson lines and field-strength tensors. In the following sections, we will compute these soft functions to reproduce the $z \rightarrow 1$ singularities in the fragmentation functions, from which we can identify the threshold logarithms.

We note that the expression for the isotropic $^3P^{[1]}$ soft function $S_{^3P^{[1]}}(z)$ has first been found in Ref. [21] in the context of shape functions. Its first moment $\int_0^1 dz S_{^3P^{[1]}}(z)$ has been obtained in Ref. [27] for the study of infrared divergences in quarkonium LDMEs; this was also used in the analysis of universality relations for $^3P_J^{[1]}$ LDMEs in Refs. [45, 46].

We can see that in the projection of the soft function onto specific color and angular momentum states that the soft function vanishes for the color-singlet S -wave state; this is because the color trace in Eq. (32) vanishes for color singlet when we set $q = 0$. This is consistent with the fact that the gluon fragmentation function for $^3S_1^{[1]}$ state is free of singularities at $z = 1$. We also note that the Dirac trace in Eq. (31) vanishes if we use the

spin-singlet projector instead of the spin-triplet one (see, for example, Eq. (A9b) of Ref. [30]). Hence, the soft function also vanishes when the final-state $Q\bar{Q}$ is in a spin-singlet state. This is consistent with the fact that the gluon fragmentation functions for spin-singlet S -wave and P -wave states do not involve singular distributions at $z = 1$. Hence, the nonvanishing soft functions that are relevant for production of a heavy quarkonium come from the ${}^3S_1^{[8]}$, ${}^3P^{[8]}$, and ${}^3P_J^{[1]}$ states.

As we have mentioned previously, the matching coefficient of the soft factorization formula that we obtain in Eq. (26) is valid at leading order in the strong coupling. Loop corrections to this coefficient can arise from gluon attachments to the fragmenting gluon; because the fragmenting gluon has a virtuality of at least M^2 , gluon attachments to the fragmenting gluon do not produce additional singularities at $z \rightarrow 1$. Hence, while radiative corrections to the matching coefficient can in principle affect the subleading singularities, the leading singularities are completely contained in the soft function in Eq. (27) to all orders in the strong coupling. Because we are only interested in the leading threshold singularities in the fragmentation functions, we only need to consider loop corrections to the soft functions.

IV. LEADING-ORDER FRAGMENTATION FUNCTIONS IN THE SOFT APPROXIMATION

In this section, we compute the soft functions at leading nonvanishing orders in the strong coupling, and verify that the soft factorization formulas we obtained in the previous section reproduce the $z \rightarrow 1$ singularities in the leading-order fragmentation functions.

A. ${}^3S_1^{[8]}$

We first consider the ${}^3S_1^{[8]}$ channel. The leading nonvanishing contribution to the soft function comes from the g^0 terms of the adjoint Wilson lines. That is,

$$\mathcal{W}({}^3S_1^{[8]})^{cb} = \delta^{ca}\delta^{ba} + O(g) = \delta^{cb} + O(g), \quad (72)$$

so that

$$S_{{}^3S_1^{[8]}}(z) = 2\pi\delta(P^+(1-z))\delta^{cb}\delta^{cb} + O(\alpha_s) = \frac{2\pi(N_c^2 - 1)}{P^+}\delta(1-z) + O(\alpha_s), \quad (73)$$

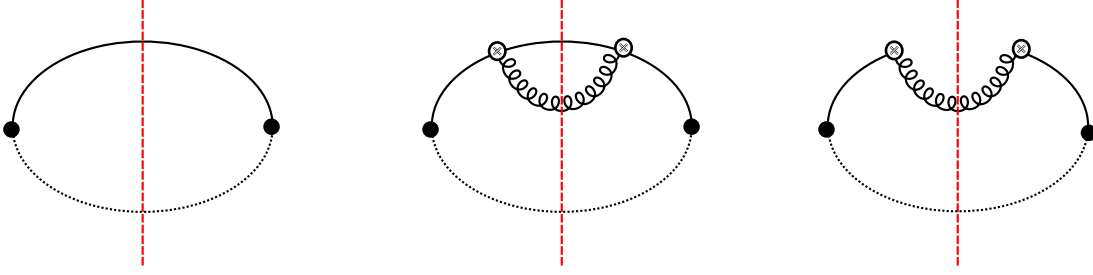


FIG. 1. Feynman diagrams for soft functions $S_{3S_1^{[8]}}(z)$ (left), $S_{3P^{[8]}}(z)$ (middle), and $S_{3P^{[1]}}(z)$ (right) at leading nonvanishing order in the strong coupling. Black solid lines are timelike Wilson lines in the p direction, dotted lines are lightlike Wilson lines in the n direction, vertical dashed lines are final-state cuts, filled circles are the spacetime origins, curly lines are gluons, and the symbol \otimes stands for insertion of the field-strength tensor.

which leads to

$$\begin{aligned} D_{g \rightarrow Q\bar{Q}(^3S_1^{[8]})}^{\text{soft}}(z) &= \frac{C_{\text{frag}}(d-2)g^2}{4m^3} \frac{2\pi 2\pi(N_c^2-1)}{P^+} \delta(1-z) + O(\alpha_s) \\ &= \frac{\pi\alpha_s}{m^3} \delta(1-z) + O(\alpha_s). \end{aligned} \quad (74)$$

By using the tree-level NRQCD matrix element $\langle 0 | \mathcal{O}^{Q\bar{Q}(^3S_1^{[8]})}(^3S_1^{[8]}) | 0 \rangle = (d-1)(N_c^2-1)$ [see Eq. (6.1c) of Ref. [33]], we obtain the $^3S_1^{[8]}$ FF in the soft approximation

$$D_{g \rightarrow Q\bar{Q}(^3S_1^{[8]})}^{\text{soft}}(z) = \frac{\pi\alpha_s}{m^3(d-1)(N_c^2-1)} \delta(1-z) + O(\alpha_s), \quad (75)$$

which agrees with the full result. As is already clear from the soft factorization formula, the $^3S_1^{[8]}$ FF for longitudinally polarized $Q\bar{Q}$ vanishes in the soft approximation, in agreement with the full result.

B. $^3P^{[8]}$

Now we consider the $^3P^{[8]}$ channel. Since the soft function $S_{3P^{[8]}}(z)$ explicitly contains the field-strength tensors, the contribution at leading nonvanishing order in α_s comes from the matrix element of $\mathcal{W}_\beta^{yx}(^3P^{[8]})$ on the vacuum and a single-gluon state. We have

$$\begin{aligned} \langle g(k) | \mathcal{W}_\beta^{yx}(^3P^{[8]}) | 0 \rangle &= \langle g(k) | \int_0^\infty d\lambda \lambda \delta^{yc} p^\mu G_{\mu\beta}^b(p\lambda) d^{bcd} \delta^{ad} \delta^{ax} | 0 \rangle + O(g^2) \\ &= i \left(\frac{i}{k \cdot p + i\varepsilon} \right)^2 p^\mu (k_\mu \delta_\beta^\alpha - k_\beta \delta_\mu^\alpha) d^{byx} + O(g^2). \end{aligned} \quad (76)$$

By squaring this we obtain

$$S_{3P^{[8]}}(z) = -(d-2) \frac{(N_c^2 - 4)(N_c^2 - 1)}{N_c} \int d\text{PS}_k \frac{2\pi(k^+ - P^+(1-z))(k \cdot p)^2}{(k \cdot p + i\varepsilon)^2(k \cdot p - i\varepsilon)^2} + O(\alpha_s), \quad (77)$$

where we used $d^{abc}d^{abc} = (N_c^2 - 4)(N_c^2 - 1)/N_c$ and $d\text{PS}_k$ is the massless phase space integral given by

$$\int d\text{PS}_k = \mu'^{2\epsilon} \int \frac{d^d k}{(2\pi)^d} 2\pi \delta(k^2) \theta(k_0), \quad (78)$$

where $\mu'^2 = \mu^2 e^{\gamma_E}/(4\pi)$ and μ is the $\overline{\text{MS}}$ scale. The phase space integral can be evaluated in light-cone coordinates as

$$\begin{aligned} & \int d\text{PS}_k \frac{2\pi(k^+ - P^+(1-z))(k \cdot p)^2}{(k \cdot p + i\varepsilon)^2(k \cdot p - i\varepsilon)^2} \\ &= \mu'^{2\epsilon} \int_0^\infty dk^+ \int_0^\infty dk^- \int \frac{d^{d-2} k_\perp}{(2\pi)^{d-2}} \frac{\delta(k^2) \delta(k^+ - P^+(1-z))}{(k \cdot p)^2} \\ &= \frac{\mu'^{2\epsilon}}{2\pi^{1-\epsilon} P_+(p^2)^{1+\epsilon}} \Gamma(1+\epsilon) \frac{1}{(1-z)^{1+2\epsilon}}. \end{aligned} \quad (79)$$

Here, we integrated over k^- and k^+ by using the delta functions, and then computed the k_\perp integral by using Eq. (C4). From this we obtain

$$S_{3P^{[8]}}(z) = -(d-2) \frac{(N_c^2 - 4)(N_c^2 - 1)}{N_c} \frac{\Gamma(1+\epsilon) \mu'^{2\epsilon}}{2\pi^{1-\epsilon} m^{2+2\epsilon} P^+} \frac{1}{(1-z)^{1+2\epsilon}} + O(\alpha_s). \quad (80)$$

This gives the fragmentation function in the soft approximation

$$D_{g \rightarrow Q\bar{Q}(^3P^{[8]})}^{\text{soft, bare}}(z) = \frac{2\alpha_s^2(N_c^2 - 4)}{3m^5 N_c} \left[1 + 2\epsilon \left(\log \frac{\mu}{2m} - \frac{1}{6} \right) + O(\epsilon^2) \right] \frac{1}{(1-z)^{1+2\epsilon}} + O(\alpha_s^3) \quad (81)$$

$$\begin{aligned} &= \frac{2\alpha_s^2(N_c^2 - 4)}{3m^5 N_c} \left[-\frac{\delta(1-z)}{2\epsilon_{\text{IR}}} + \left(\frac{1}{6} - \log \frac{\mu}{2m} \right) \delta(1-z) \right. \\ &\quad \left. + \frac{1}{(1-z)_+} + O(\epsilon) \right] + O(\alpha_s^3). \end{aligned} \quad (82)$$

In expanding the function $1/(1-z)^{1+2\epsilon}$ in powers of ϵ we used the identity

$$\frac{1}{(1-z)^{1+n\epsilon}} = -\frac{1}{n\epsilon_{\text{IR}}} \delta(1-z) + \left[\frac{1}{(1-z)^{1+n\epsilon}} \right]_+. \quad (83)$$

In NRQCD factorization, the IR pole in Eq. (81) is canceled by the one-loop correction to the ${}^3S_1^{[8]}$ matrix element, which involves both UV and IR poles. When the NRQCD matrix element is renormalized in the $\overline{\text{MS}}$ scheme, this effectively amounts to subtracting the IR pole in Eq. (81) and replacing μ by the $\overline{\text{MS}}$ scale μ_Λ . Then the renormalized result for

$D_{g \rightarrow Q\bar{Q}(^3P^{[8]})}^{\text{soft}}(z)$ is obtained by dividing by the normalization for the ${}^3P^{[8]}$ matrix element, which is given by $(d-1)(N_c^2 - 1)$ in the normalization used in Ref. [42]. We thus obtain

$$D_{g \rightarrow Q\bar{Q}(^3P^{[8]})}^{\text{soft}}(z) = \frac{8\alpha_s^2}{3(d-1)(N_c^2 - 1)m^5} \frac{N_c^2 - 4}{4N_c} \times \left[\left(\frac{1}{6} - \log \frac{\mu_\Lambda}{2m} \right) \delta(1-z) + \frac{1}{(1-z)_+} \right] + O(\alpha_s^3), \quad (84)$$

which reproduces exactly the singular distributions in the $D_{g \rightarrow Q\bar{Q}(^3P^{[8]})}(z)$. Similarly to the ${}^3S_1^{[8]}$ case, the contribution from longitudinally polarized $Q\bar{Q}$ spin vanishes in the soft approximation, which is consistent with the fact that the ${}^3P_J^{[8]}$ FF for longitudinal $Q\bar{Q}$ spin polarization does not involve singular distributions [33].

C. ${}^3P_J^{[1]}$

We next consider the ${}^3P_J^{[1]}$ channel. Similarly to the ${}^3P^{[8]}$ case, the contribution at leading nonvanishing order in α_s comes from the matrix element of $\mathcal{W}_\beta^b({}^3P_J^{[1]})$ on the vacuum and a single-gluon state. We have

$$\begin{aligned} \langle g(k) | \mathcal{W}_\beta^b({}^3P_J^{[1]}) | 0 \rangle &= \langle g(k) | \int_0^\infty d\lambda \lambda p^\sigma G_{\sigma\beta}^d(p\lambda) \delta^{da} \delta^{ba} | 0 \rangle + O(g^2) \\ &= i \left(\frac{i}{k \cdot p + i\varepsilon} \right)^2 p^\mu (k_\mu \delta_\beta^\alpha - k_\beta \delta_\mu^\alpha) \delta^{zb} + O(g^2), \end{aligned} \quad (85)$$

which leads to

$$S_{{}^3P^{[1]}}(z) = -(d-2)(N_c^2 - 1) \int dPS_k \frac{2\pi\delta(k^+ - P^+(1-z))}{(k \cdot p)^2} + O(\alpha_s), \quad (86)$$

$$\begin{aligned} S_{{}^3P^{[1]}}^{TT}(z) &= -(N_c^2 - 1) \int dPS_k \frac{2\pi\delta(k^+ - P^+(1-z))}{(k \cdot p)^2} \\ &\quad \times \left(\frac{p^2}{p_+^2} \frac{k_+^2 p^2 - 2p^+ k^+ k \cdot p}{(k \cdot p)^2} + \frac{d-2}{d-1} \right) + O(\alpha_s). \end{aligned} \quad (87)$$

It is clear from this expression that at leading nonvanishing order in α_s , $S_{{}^3P^{[1]}}(z)$ is obtained from $S_{{}^3P^{[8]}}(z)$ by multiplying $N_c/(N_c^2 - 4)$. The anisotropic part $S_{{}^3P^{[1]}}^{TT}(z)$ can again be computed in light-cone coordinates. The result is

$$\begin{aligned} S_{{}^3P^{[1]}}^{TT}(z) &= \frac{(N_c^2 - 1)\epsilon(1-\epsilon)(1-2\epsilon)\Gamma(1+\epsilon)\mu^{r2\epsilon}}{3(3-2\epsilon)\pi^{1-\epsilon}m^2P^+(1-z)^{1+2\epsilon}} + O(\alpha_s) \\ &= -\frac{N_c^2 - 1}{18\pi m^2 P^+} \delta(1-z) + O(\epsilon, \alpha_s). \end{aligned} \quad (88)$$

Because of the explicit factor of ϵ , the $S_{3P^{[1]}}^{TT}(z)$ is free of poles at leading nonvanishing order in α_s . From these we obtain

$$D_{g \rightarrow Q\bar{Q}(^3P_J^{[1]})}^{\text{soft, bare}}(z) = \frac{4\alpha_s^2}{3m^5 N_c} c^J \left[1 + 2\epsilon \left(\log \frac{\mu}{2m} - \frac{Q_J}{2J+1} \right) + O(\epsilon^2) \right] \frac{1}{(1-z)^{1+2\epsilon}} + O(\alpha_s^3) \quad (89)$$

$$= \frac{4\alpha_s^2}{3m^5 N_c} c^J \left[-\frac{\delta(1-z)}{2\epsilon_{\text{IR}}} + \left(\frac{Q_J}{2J+1} - \log \frac{\mu}{2m} \right) \delta(1-z) \right. \\ \left. + \frac{1}{(1-z)_+} + O(\epsilon) \right] + O(\alpha_s^3), \quad (90)$$

where we used $-2\epsilon(1-z)^{-1-2\epsilon} = 1 + O(\epsilon)$ to combine the order- ϵ coefficient of $(1-z)^{-1-2\epsilon}$ in $S_{3P^{[1]}}(z)$ and the finite piece in $S_{3P^{[1]}}^{TT}(z)$ into $Q_J/(2J+1)$. Here the ϵ dependence in the overall factor c_J is kept, because this corresponds to the d -dimensional definition of the $^3P_J^{[1]}$ matrix element. In the polarized case, we obtain

$$D_{g \rightarrow Q\bar{Q}(^3P_{J,h}^{[1]})}^{\text{soft, bare}}(z) = \frac{4\alpha_s^2}{3m^5 N_c} c^{J,h} \left[1 + 2\epsilon \left(\log \frac{\mu}{2m} - \frac{c^J}{c^{J,h}} \frac{Q_{J,h}}{2J+1} \right) + O(\epsilon^2) \right] \frac{1}{(1-z)^{1+2\epsilon}} + O(\alpha_s^3) \quad (91)$$

$$= \frac{4\alpha_s^2}{3m^5 N_c} c^{J,h} \left[-\frac{\delta(1-z)}{2\epsilon_{\text{IR}}} + \left(\frac{c^J}{c^{J,h}} \frac{Q_{J,h}}{2J+1} - \log \frac{\mu}{2m} \right) \delta(1-z) \right. \\ \left. + \frac{1}{(1-z)_+} + O(\epsilon) \right] + O(\alpha_s^3), \quad (92)$$

where $Q_{J=1,|h|=1} = 0$, $Q_{J=1,h=0} = 3/8$, $Q_{J=2,h=|2|} = 3/4$, $Q_{J=2,|h|=1} = 0$, and $Q_{J=2,h=0} = 1/8$. Again, the ϵ dependences in the $c^{J,h}$ are kept, because they correspond to the d -dimensional definition of the polarized $^3P_J^{[1]}$ matrix element. Similarly to the $^3P^{[8]}$ case, the IR pole is canceled by the one-loop correction to the $^3S_1^{[8]}$ matrix element, which involves an IR pole proportional to the tree-level $^3P_J^{[1]}$ matrix element. The $^3P_J^{[1]}$ short-distance coefficient in the soft approximation is then obtained by subtracting the IR pole multiplied by the normalization of the $^3P_J^{[1]}$ matrix element that is proportional to c^J ($c^{J,h}$ in the polarized case), replacing μ by the $\overline{\text{MS}}$ scale μ_Λ for renormalization of the $^3S_1^{[8]}$ matrix element, and dividing by the normalization $c_J \times 2N_c(d-1)$ of the polarization-summed $^3P_J^{[1]}$ matrix element. We obtain

$$D_{g \rightarrow Q\bar{Q}(^3P_J^{[1]})}^{\text{soft}}(z) = \frac{4\alpha_s^2}{3(d-1)m^5 N_c^2} \left[\left(\frac{Q_J}{2J+1} - \log \frac{\mu_\Lambda}{2m} \right) \delta(1-z) + \frac{1}{(1-z)_+} \right] + O(\alpha_s^3), \quad (93)$$

which reproduces exactly the singular distributions in $D_{g \rightarrow Q\bar{Q}(^3P_J^{[1]})}(z)$. Similarly, in the polarized case, we obtain

$$D_{g \rightarrow Q\bar{Q}(^3P_{J,h}^{[1]})}^{\text{soft}}(z) = \frac{4\alpha_s^2}{3(d-1)m^5N_c^2} \left[\left(\frac{Q_{J,h}}{2J+1} - a_{J,h} \log \frac{\mu_\Lambda}{2m} \right) \delta(1-z) + \frac{a_{J,h}}{(1-z)_+} \right] + O(\alpha_s^3). \quad (94)$$

where $a_{J,h} = c^{J,h}/c^J|_{d=4}$. These again exactly reproduce the singular distributions in the polarized results for $D_{g \rightarrow Q\bar{Q}(^3P_{J,h}^{[1]})}(z)$ in Refs. [39, 41], which are shown in Appendix B.

D. Summary of leading-order results

We computed the fragmentation functions in the soft approximation by using the soft factorization formulas we obtained in Sec. III. The results in Eqs. (75), (84), and (93) reproduce exactly the singular distributions, namely, the Dirac delta functions and plus distributions, in the leading-order fragmentation functions in Eqs. (4). This implies that in Mellin space,

$$\lim_{N \rightarrow \infty} \left[\tilde{D}_{g \rightarrow Q\bar{Q}(\mathcal{N})}^{\text{soft}}(N) - \tilde{D}_{g \rightarrow Q\bar{Q}(\mathcal{N})}(N) \right] = 0, \quad (95)$$

meaning that the terms in $D_{g \rightarrow Q\bar{Q}(\mathcal{N})}(z)$ that are not reproduced by the soft approximation are regular functions in z . This explicitly confirms the validity of the soft factorization at leading nonvanishing order in α_s .

V. SOFT FUNCTIONS AT NLO

In this section, we compute the soft functions that appear in the soft factorization formulas for the $^3S_1^{[8]}$, $^3P^{[8]}$, and $^3P_J^{[1]}$ fragmentation functions at NLO in α_s . We work in the Feynman gauge.

A. $^3S_1^{[8]}$

1. Real diagrams

We first consider the real diagrams, where a gluon attaches to the lightlike or timelike Wilson lines. The matrix element of $\mathcal{W}(^3S_1^{[8]})^{cb}$ on the vacuum and the one-gluon state is

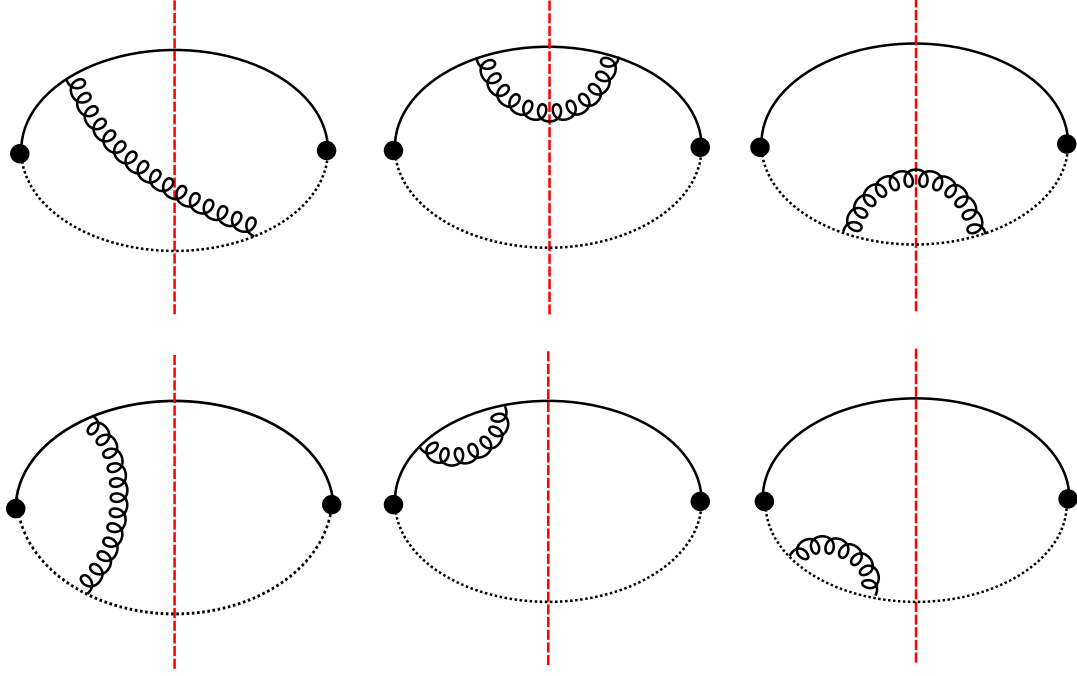


FIG. 2. Feynman diagrams that appear in NLO calculation of the soft function $S_{^3S_1^{[8]}}(z)$. There are additional diagrams that can be obtained by complex conjugation.

given at leading nonvanishing order by

$$\langle g(k) | \mathcal{W}(^3S_1^{[8]})^{cb} | 0 \rangle = -g \frac{ip \cdot \epsilon^*(k)}{k \cdot p + i\varepsilon} f^{xca} \delta^{ba} - g \frac{in \cdot \epsilon^*(k)}{k \cdot n + i\varepsilon} f^{xba} \delta^{ca} + O(g^3), \quad (96)$$

where $\epsilon(k)$ is the polarization vector of the outgoing gluon. Then the contribution from the real diagrams to $S_{^3S_1^{[8]}}(z)$ is given by

$$S_{^3S_1^{[8]}}^{\text{NLO}}(z) \Big|_{\text{real}} = g^2 C_A (N_c^2 - 1) \int d\text{PS}_k 2\pi \delta(k^+ - P^+(1-z)) \left[-\frac{p^2}{(k \cdot p)^2} + \frac{2p^+}{k^+ k \cdot p} \right]. \quad (97)$$

Here the first term in the square brackets comes from the square of the first term on the right-hand side of Eq. (96), and the second term comes from the cross term. The square of the second term on the right-hand side of Eq. (96) vanishes because it is proportional to $n^2 = 0$. The phase-space integration is straightforward:

$$\int d\text{PS}_k \frac{2\pi \delta(k^+ - P^+(1-z)) p^2}{(k \cdot p)^2} = \frac{\mu'^{2\epsilon}}{(2\pi)^{1-\epsilon} [P_+(1-z)]^{1+2\epsilon}} \Gamma(1 + \epsilon), \quad (98)$$

$$\int d\text{PS}_k \frac{2\pi \delta(k^+ - P^+(1-z)) 2p^+}{k^+ (k \cdot p)} = \frac{\mu'^{2\epsilon}}{(2\pi)^{1-\epsilon} [P_+(1-z)]^{1+2\epsilon}} \Gamma(\epsilon_{\text{UV}}), \quad (99)$$

which give

$$S_{3S_1^{[8]}}^{\text{NLO}}(z) \Big|_{\text{real}} = 4\pi\alpha_s C_A (N_c^2 - 1) \frac{\mu'^{2\epsilon}}{(2\pi)^{1-\epsilon} [P_+(1-z)]^{1+2\epsilon}} [\Gamma(\epsilon_{\text{UV}}) - \Gamma(1+\epsilon)] \quad (100)$$

$$= \frac{\alpha_s C_A (N_c^2 - 1)}{P_+} \left(\frac{\mu}{2m} \right)^{2\epsilon} \left[\frac{2}{\epsilon_{\text{UV}}} - 2 + \frac{\pi^2}{6} \epsilon + O(\epsilon^2) \right] \\ \times \left\{ -\frac{\delta(1-z)}{2\epsilon_{\text{IR}}} + \left[\frac{1}{(1-z)^{1+2\epsilon}} \right] \right\}. \quad (101)$$

2. Virtual diagrams

The contribution from the virtual diagrams that come from the exchange of a gluon between the lightlike and timelike Wilson lines is

$$S_{3S_1^{[8]}}^{\text{NLO}}(z) \Big|_{\text{virtual}} = 2\text{Re} \int_k \left(-gn^\mu \frac{i}{k \cdot n + i\varepsilon} f^{xba} \right) \frac{-ig_{\mu\nu}\delta^{bc}}{k^2 + i\varepsilon} \\ \times \left(-gp^\nu \frac{i}{-k \cdot p + i\varepsilon} f^{xca} \right) 2\pi\delta(P^+(1-z)) \\ = \text{Re} ig^2 (N_c^2 - 1) C_A \int_k \frac{2\pi\delta(1-z)}{(k^2 + i\varepsilon)(k \cdot n + i\varepsilon)(-k \cdot p + i\varepsilon)}. \quad (102)$$

We use the shorthand

$$\int_k = \mu'^{2\epsilon} \int \frac{d^d k}{(2\pi)^d}. \quad (103)$$

It is easy to compute this scaleless one-loop integral by using Schwinger parametrization. We have

$$\int_k \frac{1}{(k^2 + i\varepsilon)(k \cdot n + i\varepsilon)(-k \cdot p + i\varepsilon)} \\ = \int_0^\infty dx dy dz \int_k \exp(xk^2 + yk \cdot n - zk \cdot p + i\varepsilon) \\ = \int_0^\infty dx dy dz \int_k \exp \left(xk^2 - \frac{(ny - zp)^2}{4x} + i\varepsilon \right) \\ = \frac{i\mu'^{2\epsilon}}{(4\pi)^{d/2}} \int_0^\infty dx dy dz x^{-d/2} \exp \left(-\frac{(ny - zp)^2}{4x} \right) \\ = \frac{i}{(4\pi)^2} \frac{1}{p_+} \frac{1}{\epsilon_{\text{UV}}} \left(\frac{1}{\epsilon_{\text{IR}}} - \frac{1}{\epsilon_{\text{UV}}} \right), \quad (104)$$

which gives

$$S_{3S_1^{[8]}}^{\text{NLO}}(z) \Big|_{\text{virtual}} = \frac{\alpha_s C_A (N_c^2 - 1)}{P_+} \delta(1-z) \frac{1}{\epsilon_{\text{UV}}} \left(\frac{1}{\epsilon_{\text{IR}}} - \frac{1}{\epsilon_{\text{UV}}} \right). \quad (105)$$

The remaining diagrams have to do with the self energies of the lightlike and timelike Wilson lines. The self-energy diagram for the lightlike Wilson line vanishes in Feynman gauge because it is proportional to $n^2 = 0$. The self energy of the eikonal line gives the following correction term in the eikonal-line propagator

$$\frac{i}{l \cdot p + i\varepsilon} \left[g^2 \int_k \frac{i}{(k+l) \cdot p + i\varepsilon} f^{bcx} f^{bxa} \frac{-ip^2}{k^2 + i\varepsilon} \right] \frac{i}{l \cdot p + i\varepsilon} \equiv \frac{i}{l \cdot p + i\varepsilon} \Sigma_p(l \cdot p) \frac{i}{l \cdot p + i\varepsilon}. \quad (106)$$

This gives the field renormalization of the eikonal-line propagator

$$\frac{i}{l \cdot p - i\Sigma_p(l \cdot p) + i\varepsilon} = \frac{i}{l \cdot p + i\varepsilon} \left[1 - i \frac{\partial}{\partial l \cdot p} \Sigma_p(l \cdot p) \right]_{l \cdot p=0}^{-1} + \dots, \quad (107)$$

where the \dots are terms regular at $l \cdot p = 0$. The calculation of $\Sigma_p(l \cdot p)$ is straightforward. By using Feynman parametrization we obtain

$$\begin{aligned} \Sigma_p(l \cdot p) &= -C_A g^2 p^2 \int_k \frac{1}{(k+l) \cdot p + i\varepsilon} \frac{1}{k^2 + i\varepsilon} \\ &= -C_A g^2 p^2 \frac{i}{(4\pi)^{2-\epsilon}} \Gamma(\epsilon_{\text{UV}}) \int_0^\infty dx \frac{1}{[x^2 p^2 / 4 - xl \cdot p - i\varepsilon]^\epsilon}, \quad (108) \\ -i \frac{\partial}{\partial l \cdot p} \Sigma_p(l \cdot p) \Big|_{l \cdot p=0} &= -C_A g^2 p^2 \frac{1}{(4\pi)^{2-\epsilon}} \Gamma(\epsilon_{\text{UV}}) \int_0^\infty dx \frac{4^{1+\epsilon} \epsilon x}{(x^2 p^2)^{1+\epsilon}} \\ &= -C_A g^2 (p^2)^{-\epsilon} \frac{4^{1+\epsilon}}{(4\pi)^{2-\epsilon}} \Gamma(1+\epsilon) \int_0^\infty dx \frac{1}{x^{1+2\epsilon}} \\ &= -\frac{\alpha_s C_A}{\pi} \left(\frac{1}{2\epsilon_{\text{UV}}} - \frac{1}{2\epsilon_{\text{IR}}} \right). \quad (109) \end{aligned}$$

Hence, the self-energy diagrams give the following contribution to the ${}^3S_1^{[8]}$ soft function

$$\begin{aligned} S_{{}^3S_1^{[8]}}^{\text{NLO}}(z) \Big|_{\text{self-energy}} &= \frac{\alpha_s C_A}{\pi} \left(\frac{1}{2\epsilon_{\text{UV}}} - \frac{1}{2\epsilon_{\text{IR}}} \right) S_{{}^3S_1^{[8]}}^{\text{LO}}(z) \\ &= \frac{\alpha_s C_A (N_c^2 - 1)}{P^+} \delta(1-z) \left(\frac{1}{\epsilon_{\text{UV}}} - \frac{1}{\epsilon_{\text{IR}}} \right). \quad (110) \end{aligned}$$

3. Results and discussion

The ${}^3S_1^{[8]}$ soft function at NLO is given by the sum of Eqs. (100), (105), and (110). The result is

$$\begin{aligned} S_{{}^3S_1^{[8]}}^{\text{NLO}}(z) &= \frac{\alpha_s C_A (N_c^2 - 1)}{P^+} \left(\frac{\mu}{2m} \right)^{2\epsilon} \left[\frac{2\epsilon_{\text{UV}}^{-1} - 2 + \epsilon\pi^2/6 + O(\epsilon^2)}{(1-z)^{1+2\epsilon}} \right. \\ &\quad \left. - \delta(1-z) \frac{1}{\epsilon_{\text{UV}}} \left(\frac{1}{\epsilon_{\text{UV}}} - \frac{1}{\epsilon_{\text{IR}}} \right) + \delta(1-z) \left(\frac{1}{\epsilon_{\text{UV}}} - \frac{1}{\epsilon_{\text{IR}}} \right) \right]. \quad (111) \end{aligned}$$

The term involving $(1-z)^{-1-2\epsilon}$ comes from the real diagram, while the terms proportional to $\epsilon_{\text{UV}}^{-1} - \epsilon_{\text{IR}}^{-1}$ come from the virtual and self-energy diagrams. By using the expansion of $(1-z)^{-1-2\epsilon}$ in powers of ϵ given by

$$\frac{1}{(1-z)^{1+2\epsilon}} = -\frac{\delta(1-z)}{2\epsilon_{\text{IR}}} + \frac{1}{(1-z)_+} + \epsilon \left[\frac{-2\log(1-z)}{1-z} \right]_+ + O(\epsilon^2), \quad (112)$$

it is straightforward to see that all IR poles cancel in $S_{3S_1^{[8]}}^{\text{NLO}}(z)$. In particular, the mixed double pole $\epsilon_{\text{UV}}^{-1}\epsilon_{\text{IR}}^{-1}$ cancels between the real and virtual diagram contributions. The single IR pole $\epsilon_{\text{IR}}^{-1}$ cancels between the real and self-energy diagram contributions. By using $S_{3S_1^{[8]}}^{\text{LO}}(z) = 2\pi(N_c^2 - 1)\delta(1-z)/P^+$, we can write

$$\begin{aligned} S_{3S_1^{[8]}}(z) = & \frac{2\pi(N_c^2 - 1)}{P^+} \left(\frac{\mu}{2m} \right)^{2\epsilon} \left\{ \delta(1-z) + \frac{\alpha_s C_A}{\pi} \left[-\frac{\delta(1-z)}{2\epsilon_{\text{UV}}^2} \right. \right. \\ & + \frac{1}{\epsilon_{\text{UV}}} \left[\frac{1}{(1-z)_+} + \frac{1}{2}\delta(1-z) \right] \\ & \left. \left. + \left[\frac{-2\log(1-z)}{1-z} \right]_+ - \frac{1}{(1-z)_+} - \frac{\pi^2}{24}\delta(1-z) \right] \right\} + O(\epsilon, \alpha_s^2). \end{aligned} \quad (113)$$

Note that now all poles are of UV origin. The order- ϵ^0 term $\alpha_s C_A/\pi[-2\log(1-z)/(1-z)]_+$ is exactly the threshold double logarithmic term that appears in the NLO correction to the gluon fragmentation function in the ${}^3S_1^{[8]}$ channel. Its origin can be traced back to the order- ϵ term in the expansion of $(1-z)^{-1-2\epsilon}$ in powers of ϵ . Because of this, the coefficient of the threshold double logarithm is tied to the double UV pole, and also to the term proportional to $1/(1-z)_+$ in the single UV pole. We also note that the order- ϵ^0 term $-\alpha_s C_A/\pi \times 1/(1-z)_+$ is exactly the threshold single logarithmic term in $D_{g \rightarrow Q\bar{Q}({}^3S_1^{[8]})}(z)$ at the factorization scale $\mu_F = 2m$, which comes from the $2C_A z/(1-z)_+$ term in $P_{gg}(z)$. Similarly to the threshold double logarithm, its coefficient is tied to the $\delta(1-z)$ term in the single UV pole. Hence, the threshold logarithm in the gluon fragmentation function in the ${}^3S_1^{[8]}$ channel is determined by the coefficient of the single UV pole of the soft function, which corresponds to its anomalous dimension. To see this more clearly for the threshold double logarithm, let us take the Mellin transform and consider its large N behavior. We have

$$\tilde{S}_{3S_1^{[8]}}(N)|_{\text{threshold}} = \frac{2\pi(N_c^2 - 1)}{P^+} \left[1 + \frac{\alpha_s C_A}{\pi} \left(-\log^2 N + \frac{\log N}{\epsilon_{\text{UV}}} - \frac{1}{2\epsilon_{\text{UV}}^2} \right) \right] + O(\alpha_s^2), \quad (114)$$

where at each order in α_s we only kept the leading terms at large N . We may identify the coefficient of the $1/\epsilon_{\text{UV}}$ pole as the cusp anomalous dimension in the adjoint representation at leading order in α_s .

B. ${}^3P^{[8]}$

We now turn to the case of the ${}^3P^{[8]}$ channel. The calculation of the ${}^3P^{[8]}$ soft function is a lot more involved compared to the ${}^3S_1^{[8]}$ case, as the operator definition of $S_{{}^3P^{[8]}}(z)$ explicitly contain gluon field operators, and it already involves an IR pole at leading nonvanishing order in α_s . Fortunately, the amount of calculation needed is reduced significantly if we only consider the threshold double logarithmic contributions. As we will see later, because nonvanishing contributions to the ${}^3P^{[8]}$ soft function always involve at least one gluon crossing the cut, the loop integrals involve only the scale $P^+(1 - z)$, so that from dimensional considerations the next-to-leading order results are proportional to $(1 - z)^{-1-4\epsilon}$. Hence, the threshold double logarithmic contributions can only arise from terms proportional to $\epsilon^{-2}(1 - z)^{-1-4\epsilon}$, and so we can only retain contributions that produce double poles in ϵ . Similarly to the ${}^3S_1^{[8]}$ case, the ${}^3P^{[8]}$ soft function can be regarded as the NRQCD matrix element of the ${}^3S_1^{[8]}$ operator on the ${}^3P^{[8]}$ state at leading power in the nonrelativistic expansion, when the delta function $2\pi\delta(n \cdot \hat{p} - P^+(1 - z))$ is replaced with unity. That is, the soft function integrated over the unbounded momentum $\ell^+ \equiv P^+(1 - z)$ is proportional to the NRQCD matrix element. The next-to-leading order correction to the ${}^3S_1^{[8]}$ operator on the ${}^3P^{[8]}$ state is known to involve only a single IR pole³. This means that, because integration over ℓ^+ does not change the infrared behavior, the double pole in the soft function must be of ultraviolet nature. This significantly simplifies the calculation, as for the purpose of identifying threshold double logarithms, it suffices to look only for UV poles.

1. Planar diagrams

From the per-diagram results available in Ref. [44], we know that the double UV pole arises from the diagram where an additional virtual gluon is exchanged between the timelike and lightlike Wilson lines. The virtual correction gives the following contribution to the

³ The double poles in Eqs. (3.9) and (3.10) in Ref. [18] are coming from the vacuum polarization correction to the matrix element.

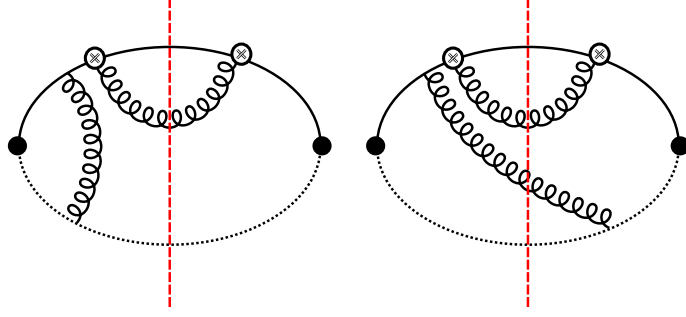


FIG. 3. Planar Feynman diagrams that appear in NLO calculation of the soft function $S_{3P[8]}(z)$. There are additional diagrams that can be obtained by complex conjugation.

matrix element of the operator $\mathcal{W}_\beta^{yx}(^3P^{[8]})$ between the vacuum and the one-gluon state:

$$\begin{aligned} & \langle g^{b,\alpha}(l) | \mathcal{W}_\beta^{yx}(^3P^{[8]}) | 0 \rangle |_{\text{virtual}} \\ &= ig^2 C_A d^{bxy} p^\mu (l_\mu \delta_\beta^\alpha - l_\beta \delta_\mu^\alpha) \int_k \frac{-i}{k^2 + i\varepsilon} p \cdot n \frac{i}{-k \cdot n + i\varepsilon} \\ & \quad \times \left[\left(\frac{i}{l \cdot p + i\varepsilon} \right)^2 \frac{i}{(l+k) \cdot p + i\varepsilon} + \frac{i}{l \cdot p + i\varepsilon} \left(\frac{i}{(l+k) \cdot p + i\varepsilon} \right)^2 \right], \end{aligned} \quad (115)$$

where b and α are the color and Lorentz indices of the outgoing gluon, respectively. Note the squaring of the timelike Wilson-line denominators, which follows from expanding the Wilson lines in the $p+q$ and $p-q$ directions to linear power in q . As we will see later, only the first term in the square brackets involves UV divergences. We thus need to compute the one-loop integral

$$I(l) = p \cdot n \int_k \frac{-i}{k^2 + i\varepsilon} \frac{i}{-k \cdot n + i\varepsilon} \frac{i}{(l+k) \cdot p + i\varepsilon} \quad (116)$$

This integral is computed straightforwardly by using the parametrization

$$\frac{1}{ABC} = \int_0^\infty dx dy \frac{2}{(A + xB + yC)^3}, \quad (117)$$

which leads to

$$\begin{aligned} I(l) &= 2ip \cdot n \int_k \int_0^\infty dx dy \frac{1}{[k^2 - xk \cdot n + y(l+k) \cdot p + i\varepsilon]^3} \\ &= \frac{p \cdot n \mu^{2\epsilon}}{(4\pi)^{2-\epsilon}} \Gamma(1+\epsilon) \int_0^\infty dx dy \frac{1}{[-xyn \cdot p/2 + yp^2(y - 4l \cdot p/p^2)/4 - i\varepsilon]^{1+\epsilon}}. \end{aligned} \quad (118)$$

We first integrate over x to obtain

$$I(l) = -\frac{\mu'^{2\epsilon} 2^{1+2\epsilon}}{(4\pi)^{2-\epsilon} (p^2)^\epsilon} \Gamma(\epsilon_{\text{UV}}) \int_0^\infty dy \frac{(y - 4l \cdot p/p^2 - i\epsilon)^{-\epsilon}}{y^{1+\epsilon}}, \quad (119)$$

where we used $\int_0^\infty dx (x+a)^{-1-\epsilon} = a^{-\epsilon} \epsilon_{\text{UV}}^{-1}$, which is valid for complex a . The integral over y yields

$$I(l) = -\frac{\mu'^{2\epsilon}}{(4\pi)^{2-\epsilon}} 2^{1-2\epsilon} (p^2)^\epsilon (l \cdot p)^{-2\epsilon} \times \Gamma(\epsilon_{\text{UV}}) \left[\frac{\Gamma(1-\epsilon)\Gamma(2\epsilon_{\text{UV}})}{\Gamma(1+\epsilon)} + \frac{e^{i\pi\epsilon} 2^{2\epsilon} \Gamma(1/2)\Gamma(-\epsilon_{\text{IR}})}{\Gamma(1/2-\epsilon)} \right], \quad (120)$$

where the first term in the square brackets comes from the region $y > 4l \cdot p/p^2$, while the second term comes from $0 < y < 4l \cdot p/p^2$. The factor $e^{i\pi\epsilon}$ produces imaginary parts of this integral, but since this cancels when the complex conjugated diagram is added, it may be discarded without affecting the poles of $I(l)$. By expanding the last line of Eq. (120) in powers of ϵ , we find

$$I(l) = -\frac{\mu'^{2\epsilon}}{(4\pi)^{2-\epsilon}} 2^{1-2\epsilon} (p^2)^\epsilon (l \cdot p)^{-2\epsilon} \left(\frac{1}{2\epsilon_{\text{UV}}^2} - \frac{1}{\epsilon_{\text{UV}}\epsilon_{\text{IR}}} + O(\epsilon^{-1}) \right). \quad (121)$$

The order- ϵ^{-1} terms do not affect the threshold double logarithms, and can be discarded in this work. Hence, the UV-divergent contribution of the virtual planar diagram to the soft function $S_{3P[8]}(z)$ is given by

$$S_{3P[8]}(z)|_{\text{virtual, UV}} = -g^2(d-2) \frac{(N_c-4)(N_c^2-1)}{N_c} \times C_A \int d\text{PS}_l \frac{2\pi\delta(l^+ - P^+(1-z))I(l)}{(l \cdot p)^2} + \text{c.c.}, \quad (122)$$

where c.c. denote the complex conjugation of preceding terms. The phase-space integration is almost identical to the tree-level calculation. We have

$$\int d\text{PS}_l \frac{2\pi\delta(l^+ - P^+(1-z))(p^2)^\epsilon}{(l \cdot p)^{2+2\epsilon}} = \frac{\mu'^{2\epsilon}}{2\pi^{1-\epsilon} P^+(p^2)^{1+2\epsilon}} \frac{\Gamma(1+3\epsilon)}{\Gamma(2+2\epsilon)} \frac{1}{(1-z)^{1+4\epsilon}}, \quad (123)$$

which yields

$$S_{3P[8]}(z)|_{\text{virtual, UV}} = 2g^2(d-2) \frac{(N_c-4)(N_c^2-1)}{N_c} \times C_A \frac{\mu'^{4\epsilon}}{16\pi^{3-2\epsilon} P^+(p^2)^{1+2\epsilon}} \frac{1}{(1-z)^{1+4\epsilon}} \left(\frac{1}{2\epsilon_{\text{UV}}^2} - \frac{1}{\epsilon_{\text{UV}}\epsilon_{\text{IR}}} + O(\epsilon^{-1}) \right). \quad (124)$$

The mixed double pole $1/(\epsilon_{\text{UV}}\epsilon_{\text{IR}})$ in the virtual planar diagram contribution cancels against the real diagram. To see this, it is instructive to recompute the integral $I(l)$ in light-cone coordinates, which also allows us to show that the last term in the last line of Eq. (115) does not produce double logarithms. We have

$$I(l) = i\mu'^{2\epsilon} \int_{-\infty}^{+\infty} \frac{dk^+}{2\pi} \int_{-\infty}^{+\infty} \frac{dk^-}{2\pi} \int \frac{d^{d-2}k_\perp}{(2\pi)^{d-2}} \frac{1}{(2k^+k^- - \mathbf{k}_\perp^2 + i\varepsilon)} \\ \times \frac{1}{(-k^+ + i\varepsilon)(l^+ + l^- + k^+ + k^- + i\varepsilon)}. \quad (125)$$

We first integrate over k^- by using contour integration. For $k^+ > 0$, both $k^2 + i\varepsilon$ and $(l + k) \cdot p + i\varepsilon$ denominator poles are on the same side of the real line, so that the contour integral vanishes. Hence we have

$$I(l) = \frac{\mu'^{2\epsilon}}{(2\pi)^{d-1}} \int_{-\infty}^0 dk^+ \int d^{d-2}k_\perp \frac{1}{k^+[\mathbf{k}_\perp^2 + 2k^{+2} + 2k^+(l^+ + l^-) - i\varepsilon]}. \quad (126)$$

Note that the k_\perp integral has a UV-divergent power count. If we first integrate over k_\perp , then the k^+ integral involves IR and UV poles arising from small and large $|k^+|$. The last term in the last line of Eq. (115) results in a similar integral, except that the $[\mathbf{k}_\perp^2 + 2k^{+2} + 2k^+(l^+ + l^-) - i\varepsilon]$ denominator factor is now squared. In this case, the k_\perp integral does not have a UV-divergent power count, and the integral can at most have a single pole. Since such contributions cannot produce threshold double logarithms, the last term in the last line of Eq. (115) can be discarded in this work.

By plugging the expression in Eq. (126) to Eq. (122) we obtain

$$S_{3P^{[8]}}|_{\text{virtual, UV}} = -g^2(d-2) \frac{(N_c^2 - 4)(N_c^2 - 1)}{N_c} \\ \times \frac{C_A \mu'^{2\epsilon}}{(2\pi)^{2d-3}(p_+)^2} \int_0^\infty dl^+ \int_0^\infty dl^- \int d^{d-2}l_\perp \int_{-\infty}^0 dk^+ \int d^{d-2}k_\perp \\ \times \frac{\delta(l_+ - P^+(1-z))\delta(l^2)}{k_+(l_+ + l_-)^2[\mathbf{k}_\perp^2 + 2k_+^2 + 2k_+(l_+ + l_-) - i\varepsilon]} + \text{c.c.} \quad (127)$$

Now we consider the corresponding real diagram. The matrix element of the operator $\mathcal{W}_\beta^{yx}(3P^{[8]})$ between the vacuum and a two-gluon state from the gluon attachment on the timelike Wilson line is given by

$$\langle g^{a_1, \mu_1}(k_1) g^{a_2, \mu_2}(k_2) | \mathcal{W}_\beta^{yx}(3P^{[8]}) | 0 \rangle|_{\text{real (a)}} \\ = -ig \left[\frac{i}{p \cdot k_1 + i\varepsilon} \left(\frac{i}{p \cdot (k_1 + k_2) + i\varepsilon} \right)^2 + \left(\frac{i}{p \cdot k_1 + i\varepsilon} \right)^2 \frac{i}{p \cdot (k_1 + k_2) + i\varepsilon} \right] \\ \times p^\mu (k_{1\mu} \delta_\beta^{\mu_1} - k_{1\beta} \delta_\mu^{\mu_1}) p^{\mu_2} d^{a_1 yd} f^{a_2 dx}. \quad (128)$$

The one from the gluon attachment on the lightlike Wilson line is

$$\begin{aligned} & \langle g^{a_1, \mu_1}(k_1) g^{a_2, \mu_2}(k_2) | \mathcal{W}_\beta^{yx}(^3P^{[8]}) | 0 \rangle |_{\text{real (b)}} \\ &= -ig \frac{i}{n \cdot k_2 + i\varepsilon} \left(\frac{i}{p \cdot k_1 + i\varepsilon} \right)^2 p^\mu (k_{1\mu} \delta_\beta^{\mu_1} - k_{1\beta} \delta_\mu^{\mu_1}) n^{\mu_2} d^{a_1 dy} f^{a_2 xd}. \end{aligned} \quad (129)$$

Similarly to the virtual diagram, only the first term in the square brackets in Eq. (128) will give rise to a UV-divergent power count, so that the remaining term can be discarded. The UV-divergent contribution to $S_{^3P^{[8]}}(z)$ from the planar real diagram is then given by

$$\begin{aligned} S_{^3P^{[8]}}(z) |_{\text{real, UV}} &= - \int dPS_{k_1} \int dPS_{k_2} 2\pi \delta(k_1^+ + k_2^+ - P^+(1-z)) \\ &\quad \times g^2(d-2) \frac{(N_c^2 - 1)(N_c^2 - 4)}{N_c} \frac{C_A p^+}{k_2^+ (k_1 \cdot p)^2 [(k_1 + k_2) \cdot p]} + \text{c.c.} \\ &= -g^2(d-2) \frac{(N_c^2 - 1)(N_c^2 - 4)}{N_c} \\ &\quad \times \frac{C_A \mu'^{2\epsilon}}{(2\pi)^{2d-3} (p^+)^2} \int_0^\infty dl^+ \int_0^\infty dl^- \int d^{d-2} l_\perp \int_0^\infty dk^+ \int_0^\infty dk^- \int d^{d-2} k_\perp \\ &\quad \times \frac{\delta(l^+ + k^+ - P^+(1-z)) \delta(l^2) \delta(k^2)}{k^+ (l^+ + l^-)^2 (l^+ + l^- + k^+ + k^-)} + \text{c.c.} \\ &= -g^2(d-2) \frac{(N_c^2 - 1)(N_c^2 - 4)}{N_c} \\ &\quad \times \frac{C_A \mu'^{2\epsilon}}{(2\pi)^{2d-3} (p^+)^2} \int_0^\infty dl^+ \int_0^\infty dl^- \int d^{d-2} l_\perp \int_0^\infty dk^+ \int d^{d-2} k_\perp \\ &\quad \times \frac{\delta(l^+ + k^+ - P^+(1-z)) \delta(l^2)}{k^+ (l^+ + l^-)^2 [k_\perp^2 + 2k^{+2} + 2k^+ (l^+ + l^-)]} + \text{c.c.}, \end{aligned} \quad (130)$$

where in the second equality we relabeled momenta k_1 and k_2 as l and k to allow direct comparison with the expression in Eq. (127), and in the last equality we integrated over k^- by using $\delta(k^2)$. It is now easy to see that the integrands of Eqs. (127) and (130) coalesce at $k^+ = 0$, so that the IR divergence at $k^+ \rightarrow 0$ cancels in the sum of virtual and real planar diagrams. While the k_\perp integral in Eq. (130) is UV divergent, there is no source of additional UV poles because the k^+ and l^+ are bounded, unlike the virtual diagram. Therefore, in the sum of real and virtual planar diagrams, only the double UV pole in the virtual diagram produces the threshold double logarithm. We obtain

$$\begin{aligned} S_{^3P^{[8]}}(z) |_{\text{NLO planar}} &= g^2(d-2) \frac{(N_c^2 - 4)(N_c^2 - 1)}{N_c} \\ &\quad \times C_A \frac{\mu'^{4\epsilon}}{16\pi^{3-2\epsilon} P^+ (p^2)^{1+2\epsilon}} \frac{1}{(1-z)^{1+4\epsilon}} \left(\frac{1}{\epsilon_{\text{UV}}^2} + O(\epsilon^{-1}) \right). \end{aligned} \quad (131)$$

2. UV power counting

Now we consider the remaining NLO diagrams that contribute to $S_{3P[8]}(z)$. As we have discussed previously, threshold double logarithms can only arise in $S_{3P[8]}(z)$ at NLO from double UV poles multiplying $(1-z)^{-1-n\epsilon}$. We will show in this section that none of the remaining diagrams can produce double UV poles, so that they can be discarded if we only look for threshold double logarithms.

Note that all doubly virtual diagrams vanish because they are proportional to a vanishing color factor $d^{bcd}f^{bda} = 0$, where d^{bcd} comes from the operator definition of the $\mathcal{W}_\beta^{yx}(^3P[8])$ and f^{bda} comes from the attachment of a gluon onto a Wilson line on the same side of the cut. Some virtual-real diagrams also vanish if a gluon from the field-strength tensor attaches to a Wilson line on the same side of the cut without additional vertices on the Wilson line between the gluon attachment and the field-strength tensor, because they are also proportional to the same vanishing color factor. This leaves us with only a handful of virtual-real diagrams and doubly real diagrams.

The virtual-real diagrams involve a one-loop integral, followed by a phase-space integral over a lightlike momentum ℓ . The phase-space integral cannot produce double UV poles, because the ℓ^+ and ℓ^- integrals have finite bounds, and so only the ℓ_\perp integral can produce UV poles. In practice, virtual-real diagrams can produce double UV poles only when the virtual one-loop integral contains a double UV pole. This is because, due to dimensional considerations, the phase-space integral cannot have a UV-divergent power count unless the gluon with momentum ℓ from the field-strength tensor attaches to the lightlike Wilson line on the other side of the cut, so that the phase-space integrand carries factors of $\ell \cdot n$ in the denominator; in such case, the virtual one-loop integral is UV finite because its integrand carries too many propagator denominator factors.

We have checked that, with the exception of the planar virtual diagram we computed in the previous section, all other UV-divergent virtual-real diagrams contain only single UV poles. This is clear for self-energy and vertex correction diagrams, as we know from renormalization of the QCD Lagrangian that they only involve single UV poles at one loop. The only diagram that needs attention is the one involving the triple-gluon vertex, where the additional gluon is attached to the timelike Wilson line. This diagram involves the one-loop

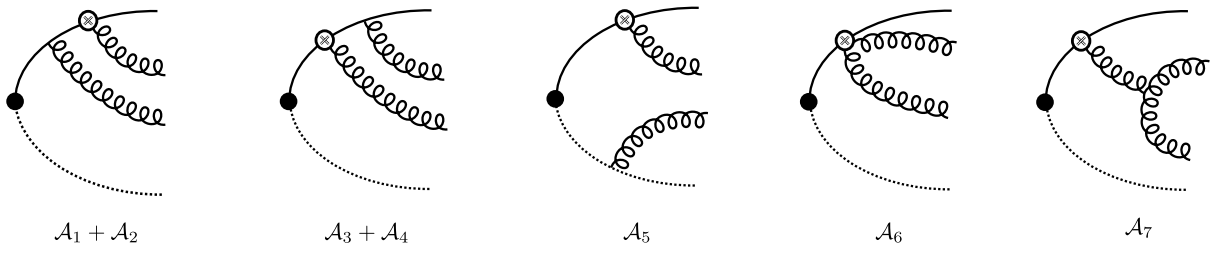


FIG. 4. Feynman diagrams for amplitudes that give rise to the doubly real contributions in the soft function $S_{3P^{[8]}}(z)$ at NLO. See Eq. (134) and text for definitions of \mathcal{A}_1 – \mathcal{A}_7 .

integral given by

$$\int_k \left[\frac{1}{\ell \cdot p (k \cdot p)^2} + \frac{1}{(\ell \cdot p)^2 k \cdot p} \right] \frac{n(k)}{k^2 (k - \ell)^2}, \quad (132)$$

where the numerator $n(k)$ is proportional to

$$\begin{aligned} & (p \cdot \ell g^{\mu\beta} - \ell^\beta p^\mu) (p \cdot k \delta_\beta^\nu - k_\beta p^\nu) p^\sigma [g_{\mu\nu}(-k - \ell)_\sigma + g_{\sigma\mu}(2\ell - k)_\nu + g_{\nu\sigma}(2k - \ell)_\mu] \\ &= (2 - d)[(\ell \cdot p)^2 k \cdot p + \ell \cdot p (k \cdot p)^2] - \frac{m^2}{2}(k - \ell)^2 (\ell \cdot p + k \cdot p) + \frac{m^2}{2} k^2 (k \cdot p - 3\ell \cdot p). \end{aligned} \quad (133)$$

It is easy to evaluate the resulting integrals with standard methods, for example by using Feynman parametrization, to confirm that none contain double UV poles, so this diagram can be discarded as well.

Now we are left with doubly real diagrams. All diagrams that contribute to the matrix element of the operator $\mathcal{W}_\beta^{yx}(^3P^{[8]})$ between the vacuum and a two-gluon state from the gluon attachment on the timelike Wilson line $\langle g^{a_1, \mu_1}(k_1) g^{a_2, \mu_2}(k_2) | \mathcal{W}_\beta^{yx}(^3P^{[8]}) | 0 \rangle$ are shown

in Fig. 4. Their values are

$$\begin{aligned} \mathcal{A}_1 + \mathcal{A}_2 &= -ig \left[\frac{i}{p \cdot k_1 + i\varepsilon} \left(\frac{i}{p \cdot (k_1 + k_2) + i\varepsilon} \right)^2 + \left(\frac{i}{p \cdot k_1 + i\varepsilon} \right)^2 \frac{i}{p \cdot (k_1 + k_2) + i\varepsilon} \right] \\ &\quad \times p^\mu (k_{1\mu} \delta_\beta^{\mu_1} - k_{1\beta} \delta_\mu^{\mu_1}) p^{\mu_2} \delta^{yc} \delta^{a_1 b} d^{bcd} f^{a_2 dx}, \end{aligned} \quad (134a)$$

$$\begin{aligned} \mathcal{A}_3 + \mathcal{A}_4 &= -ig \left[\frac{i}{p \cdot k_2 + i\varepsilon} \left(\frac{i}{p \cdot (k_1 + k_2) + i\varepsilon} \right)^2 + \left(\frac{i}{p \cdot k_2 + i\varepsilon} \right)^2 \frac{i}{p \cdot (k_1 + k_2) + i\varepsilon} \right] \\ &\quad \times p^\mu (k_{1\mu} \delta_\beta^{\mu_1} - k_{1\beta} \delta_\mu^{\mu_1}) p^{\mu_2} f^{a_2 yc} \delta^{ba_1} d^{bcd} \delta^{da} \delta^{xa}, \end{aligned} \quad (134b)$$

$$\mathcal{A}_5 = -ig \frac{i}{n \cdot k_2 + i\varepsilon} \left(\frac{i}{p \cdot k_1 + i\varepsilon} \right)^2 p^\mu (k_{1\mu} \delta_\beta^{\mu_1} - k_{1\beta} \delta_\mu^{\mu_1}) n^{\mu_2} \delta^{yc} \delta^{a_1 b} d^{bcd} f^{a_2 xd}, \quad (134c)$$

$$\mathcal{A}_6 = \frac{g}{[p \cdot (k_1 + k_2)]^2} (p^{\mu_1} \delta_\beta^{\mu_2} - p^{\mu_2} \delta_\beta^{\mu_1}) d^{bcd} f^{ba_1 a_2} \delta^{da} \delta^{xa} \delta^{yc}, \quad (134d)$$

$$\begin{aligned} \mathcal{A}_7 &= \frac{g}{[p \cdot (k_1 + k_2)]^2} \frac{1}{(k_1 + k_2)^2} p^\mu [(k_1 + k_2)^\mu \delta_\beta^\nu - (k_1 + k_2)_\beta g^{\mu\nu}] \\ &\quad \times G_3^{\nu\mu_1\mu_2}(k_1 + k_2, -k_1, -k_2) d^{bcd} f^{ba_1 a_2} \delta^{da} \delta^{xa} \delta^{yc}, \end{aligned} \quad (134e)$$

with $G_3^{\mu_1\mu_2\mu_3}(k_1, k_2, k_3) = g^{\mu_1\mu_2}(k_1 - k_2)_{\mu_3} + g^{\mu_2\mu_3}(k_2 - k_3)_{\mu_1} + g^{\mu_3\mu_1}(k_3 - k_1)_{\mu_2}$. In Eq. (134a), \mathcal{A}_1 and \mathcal{A}_2 are given by the contributions from the first and second terms in the square brackets, respectively; similarly, in Eq. (134b), \mathcal{A}_3 and \mathcal{A}_4 are given by the contributions from the first and second terms in the square brackets, respectively. The amplitude \mathcal{A}_6 comes from the $A^\mu A^\nu$ term of the field-strength tensor, while the \mathcal{A}_7 arises from the triple-gluon vertex. In \mathcal{A}_1 through \mathcal{A}_5 , the gluon attached to the field-strength tensor carries the momentum k_1 . If we define the crossed amplitudes as $\bar{\mathcal{A}}_i \equiv \mathcal{A}_i|_{1 \leftrightarrow 2}$, the contributions to $S_{3P[8]}(z)$ from the doubly real diagrams are given by $\mathcal{A}_i^* \mathcal{A}_j$ and $\mathcal{A}_i^* \bar{\mathcal{A}}_j$ for $i, j = 1, 2, \dots, 7$, multiplied by $2\pi\delta(k_1^+ + k_2^+ - P^+(1-z))$, and integrated over the phase space of k_1 and k_2 . We now examine the UV divergences in each contribution.

The calculation of the planar diagrams in the previous section leads to a simple way to analyze UV divergences in these phase-space integrals. If we evaluate a phase-space integral over k in light-cone coordinates, the only source of UV divergences is the integral over k_\perp , because the k^- integral is done by the on-shell delta function $\delta(k^2)$, and the k^+ integral has a finite bound. Hence, for doubly real diagrams where the final state involves two gluons with momenta k_1 and k_2 , it suffices to consider only the power counting of the $k_{1\perp}$ and $k_{2\perp}$ integrals, after integrating out the $\delta(k_1^2)$ and $\delta(k_2^2)$ with the k_1^- and k_2^- integrals. In most

cases, general form of the $k_{1\perp}$ and $k_{2\perp}$ integrals at large $|\mathbf{k}_{1\perp}|$ and $|\mathbf{k}_{2\perp}|$ can be written as

$$\int \frac{d^{d-2}k_{1\perp} d^{d-2}k_{2\perp}}{\mathbf{k}_{1\perp}^{2a} \mathbf{k}_{2\perp}^{2b} (\mathbf{k}_{1\perp}^2 + \mathbf{k}_{2\perp}^2)^c}, \quad (135)$$

after suitable rescaling of $k_{1\perp}$ and $k_{2\perp}$. There are exceptional cases when a factor of $k_1 \cdot k_2$ appears in the numerator or in the denominator; we will later examine these cases explicitly. We can easily identify the UV behaviors of the $k_{1\perp}$ and $k_{2\perp}$ integrals in Eq. (135) by counting the degrees of divergence. If an integral over k_\perp behaves like $\int \frac{d^{d-2}k_\perp}{\mathbf{k}_\perp^{2n}}$ at large $|\mathbf{k}_\perp|$, then the degree of divergence of this integral is $d - 2 - 2n$. If this number vanishes or exceeds 0 at $d = 4$, then the k_\perp integral can be UV divergent. Let us now apply this analysis to integrals of the form Eq. (135). The case $c = 0$ is trivial, in which case the degrees of divergence of the $k_{1\perp}$ and $k_{2\perp}$ integrals are simply given by $d - 2 - 2a$ and $d - 2 - 2b$, respectively. In the general case $c \neq 0$, if we integrate over $k_{2\perp}$ first, the degree of divergence of the $k_{2\perp}$ integral is $d - 2 - 2(b + c)$. Since the only scale of the $k_{2\perp}$ integral is $|\mathbf{k}_{1\perp}|$, the remaining $k_{1\perp}$ integral is proportional to $\int d^{d-2}k_{1\perp} |\mathbf{k}_{1\perp}|^{d-2-2(a+b+c)}$. The degree of divergence of this integral is $2(d - 2 - a - b - c)$.

Now let us examine the case where a factor of $k_1 \cdot k_2$ appears in the numerator. From

$$k_1 \cdot k_2 = k_1^+ k_2^- + k_1^- k_2^+ - \mathbf{k}_{1\perp} \cdot \mathbf{k}_{2\perp}, \quad (136)$$

after integrating out the on-shell delta functions to eliminate k_1^- and k_2^- , the first and second terms become proportional to $\mathbf{k}_{2\perp}^2$ and $\mathbf{k}_{1\perp}^2$, respectively. The last term is odd in both $k_{1\perp}$ and $k_{2\perp}$, while the remaining integrand factors are even, so that it can be discarded. Hence, integrals with a factor of $k_1 \cdot k_2$ in the numerator can always be reduced to the form in Eq. (135).

The remaining case is when the factor $k_1 \cdot k_2$ appears in the denominator. These integrals appear in the form

$$\int d\text{PS}_{k_1} \int d\text{PS}_{k_2} \frac{2\pi\delta(k_1^+ + k_2^+ - P^+(1-z))}{(k_1 \cdot p)^a (k_2 \cdot p)^b [(k_1 + k_2) \cdot p]^c k_1 \cdot k_2}. \quad (137)$$

After integration over the on-shell delta functions by eliminating k_1^- and k_2^- , the factors $k_1 \cdot p$, $k_2 \cdot p$, and $(k_1 + k_2) \cdot p$ involve $\mathbf{k}_{1\perp}^2$, $\mathbf{k}_{2\perp}^2$, and $\mathbf{k}_{1\perp}^2 + \mathbf{k}_{2\perp}^2$, respectively, while $k_1 \cdot k_2$ involves a linear combination of $\mathbf{k}_{1\perp}^2$, $\mathbf{k}_{2\perp}^2$, and $\mathbf{k}_{1\perp} \cdot \mathbf{k}_{2\perp}$. Explicit calculation shows that we never encounter cases where both a and b are positive. If $b \leq 0$ and $a \geq 0$, we can combine the $[(k_1 + k_2) \cdot p]^c$ and $k_1 \cdot k_2$ denominator factors by using Feynman parametrization and

shift $k_{2\perp}$ to eliminate the $\mathbf{k}_{1\perp} \cdot \mathbf{k}_{2\perp}$ term in the denominator. Hence, this integral reduces to the form given in Eq. (135), and the UV power counting can be done in the same way. The same applies to the case $a \leq 0$ and $b \geq 0$. The case where both a and b are negative can be rewritten as a linear combination of integrals with either $a = 0$ or $b = 0$ by using $2(k_1 \cdot p)(k_2 \cdot p) = [(k_1 + k_2) \cdot p]^2 - (k_1 \cdot p)^2 - (k_2 \cdot p)^2$. As a result, the UV power counting of all integrals of the form in Eq. (137) can be done in a similar way.

By applying the UV power counting analysis of all doubly real diagrams, we find that the only diagrams that have a UV-divergent power count are: $\mathcal{A}_2^* \mathcal{A}_5$ which is the real planar diagram we computed in the previous section, $\mathcal{A}_5^* \mathcal{A}_7$, and $\mathcal{A}_5^* \bar{\mathcal{A}}_5$. Note that the contribution from $\mathcal{A}_2^* \bar{\mathcal{A}}_4$ is proportional to a vanishing color factor, similarly to its virtual-real counterpart. Note that none of these diagrams involve double UV divergences, as only one of the $k_{1\perp}$ and $k_{2\perp}$ integrals are UV divergent. In fact, it can be shown by direct evaluation that the contributions from $\mathcal{A}_5^* \bar{\mathcal{A}}_5$ and $\mathcal{A}_5^* \mathcal{A}_7$ are actually UV finite. The diagram $\mathcal{A}_5^* \bar{\mathcal{A}}_5$ is proportional to

$$\begin{aligned} & \int d\text{PS}_{k_1} \int d\text{PS}_{k_2} \frac{k_1^+ k_2^0 + k_2^+ k_1^0 - k_1 \cdot k_2 / \sqrt{2}}{(k_1^0)^2 (k_2^0)^2 k_1^+ k_2^+} 2\pi \delta(k_1^+ + k_2^+ - P^+(1-z)) \\ &= \int d\text{PS}_{k_1} \int d\text{PS}_{k_2} \frac{k_1^+ k_2^0 + k_2^+ k_1^0 - (k_1^+ k_2^- + k_1^- k_2^+) / \sqrt{2}}{(k_1^0)^2 (k_2^0)^2 k_1^+ k_2^+} 2\pi \delta(k_1^+ + k_2^+ - P^+(1-z)) \\ &= \sqrt{2} \int d\text{PS}_{k_1} \int d\text{PS}_{k_2} \frac{2\pi \delta(k_1^+ + k_2^+ - P^+(1-z))}{(k_1^0)^2 (k_2^0)^2}, \end{aligned} \quad (138)$$

where in the first equality we eliminated the $\mathbf{k}_{1\perp} \cdot \mathbf{k}_{2\perp}$ term because it is odd in both $k_{1\perp}$ and $k_{2\perp}$, and in the second equality we used $k_{1,2}^0 = (k_{1,2}^+ + k_{1,2}^-) / \sqrt{2}$. The resulting integral is now UV finite in both $\mathbf{k}_{1\perp}$ and $\mathbf{k}_{2\perp}$.

The diagram $\mathcal{A}_5^* \mathcal{A}_7$ needs more work. If we only collect the terms that provide a UV-divergent power count, we have

$$\int d\text{PS}_{k_1} \int d\text{PS}_{k_2} \frac{k_2^0 / \sqrt{2} - k_1^+ (k_2^0)^2 / k_1 \cdot k_2}{(k_1^0)^2 k_2^+ (k_1^0 + k_2^0)^2} 2\pi \delta(k_1^+ + k_2^+ - P^+(1-z)). \quad (139)$$

If we first integrate over k_1^- and k_2^- by using the on-shell delta functions, and then integrate over $k_{2\perp}$ followed by integration over $k_{1\perp}$, only the $k_{2\perp}$ integral involves UV divergences. This means that, only the highest powers of $k_{2\perp}$ in the numerator k_2^0 , which comes from the k_2^- component, produces UV divergences. Hence, we can replace k_2^0 with $k_2^- / \sqrt{2}$ in the numerator without affecting the UV poles. We have then

$$\frac{1}{2} \int d\text{PS}_{k_1} \int d\text{PS}_{k_2} \frac{k_2^- - k_1^+ (k_2^-)^2 / k_1 \cdot k_2}{(k_1^0)^2 k_2^+ (k_1^0 + k_2^0)^2} 2\pi \delta(k_1^+ + k_2^+ - P^+(1-z)). \quad (140)$$

We can rewrite the term involving $k_1 \cdot k_2$ in the denominator as

$$\begin{aligned} & \int d\text{PS}_{k_1} \int d\text{PS}_{k_2} \frac{k_1^+(k_2^-)^2}{(k_1^0)^2 k_2^+ (k_1^0 + k_2^0)^2 k_1 \cdot k_2} 2\pi \delta(k_1^+ + k_2^+ - P^+(1-z)) \\ &= \int d\text{PS}_{k_1} \int d\text{PS}_{k_2} \frac{k_2^-(k_1 \cdot k_2 - k_1^- k_2^+ + \mathbf{k}_{1\perp} \cdot \mathbf{k}_{2\perp})}{(k_1^0)^2 k_2^+ (k_1^0 + k_2^0)^2 k_1 \cdot k_2} 2\pi \delta(k_1^+ + k_2^+ - P^+(1-z)). \end{aligned} \quad (141)$$

The $k_1^- k_2^+$ term does not have a UV-divergent power count. In the case of the $\mathbf{k}_{1\perp} \cdot \mathbf{k}_{2\perp}$ term, if we combine the denominator factors $(k_1^0 + k_2^0)^2$ and $k_1 \cdot k_2$ by using Feynman parametrization and integrate over $\mathbf{k}_{2\perp}$, the shift in $\mathbf{k}_{2\perp}$ that is necessary in eliminating the term linear in $\mathbf{k}_{2\perp}$ in the denominator will produce up to a $\mathbf{k}_{1\perp}^2$ term in the numerator, while $\mathbf{k}_{2\perp}$ disappears in the numerator. Similarly to the $k_1^- k_2^+$ term, this term does not have a UV-divergent power count. Hence, the only UV-divergent contribution comes from the $k_1 \cdot k_2$ term. Then the sum of UV-divergent contribution to this diagram can be written as

$$\frac{1}{2} \int d\text{PS}_{k_1} \int d\text{PS}_{k_2} \frac{k_2^- - k_2^+}{(k_1^0)^2 k_2^+ (k_1^0 + k_2^0)^2} 2\pi \delta(k_1^+ + k_2^+ - P^+(1-z)), \quad (142)$$

which vanishes. Hence, we conclude that the diagram $\mathcal{A}_5^* \mathcal{A}_7$ is UV finite. Therefore, the only doubly real diagram that contains a UV divergence is $\mathcal{A}_2^* \mathcal{A}_5$, which we considered in the previous section.

The analysis of the NLO diagrams in this section shows that the threshold double logarithms, which arise from double UV poles, can only arise from the planar diagrams that we considered in the previous section. While the double UV pole only appears in the virtual-real planar diagram, the cancellation of the mixed double pole requires the corresponding doubly real diagram. All other diagrams can produce at most single UV poles,

The analysis of the doubly real diagrams also serve as a double check of the virtual-real diagrams: if a doubly real diagram contains a UV pole, the corresponding virtual-real diagram can contain a double UV pole because the virtual loop integral can contain additional UV divergences that arise from the unbound k^+ integral. The non-appearance of UV divergences in doubly real diagrams other than the planar diagram we considered in the previous section is consistent with our analysis that the only double UV pole arises from the planar virtual-real diagram.

3. Results and discussion

The ${}^3P^{[8]}$ soft function at NLO is given by

$$S_{{}^3P^{[8]}}(z) = -(1-\epsilon) \frac{(N_c^2 - 4)(N_c^2 - 1)}{N_c} \frac{1}{\pi m^2 P^+} \quad (143)$$

$$\times \left[\frac{(\pi \mu'^2/m^2)^\epsilon \Gamma(1+\epsilon)}{(1-z)^{1+2\epsilon}} - \frac{\alpha_s C_A (\pi \mu'^2/m^2)^{2\epsilon}}{2\pi} \frac{\epsilon_{\text{UV}}^{-2} + O(\epsilon^{-1})}{(1-z)^{1+4\epsilon}} + O(\alpha_s^2) \right], \quad (144)$$

where we neglect contributions at order α_s that do not produce threshold double logarithms. At order α_s , the expansion in powers of ϵ produces many terms; since we are only interested in identifying the threshold double logarithms, we can discard contributions that are unrelated to leading singularities at $z \rightarrow 1$. The factor $(1-\epsilon)(\pi \mu'^2/m^2)^{2\epsilon} \epsilon_{\text{UV}}^{-2}$ gives⁴

$$(1-\epsilon)(\pi \mu'^2/m^2)^{2\epsilon} \epsilon_{\text{UV}}^{-2} = \frac{1}{\epsilon_{\text{UV}}^2} + \frac{2 \log \frac{\mu^2}{4m^2} + 2\gamma_E - 1}{\epsilon_{\text{UV}}} + O(\epsilon^0). \quad (145)$$

while the factor $(1-z)^{-1-4\epsilon}$ yields

$$\frac{1}{(1-z)^{1+4\epsilon}} = -\frac{\delta(1-z)}{4\epsilon_{\text{IR}}} + \frac{1}{(1-z)_+} - 4\epsilon \left[\frac{\log(1-z)}{1-z} \right]_+ + 8\epsilon^2 \left[\frac{\log^2(1-z)}{1-z} \right]_+ + O(\epsilon^3), \quad (146)$$

We can see that the $\epsilon_{\text{UV}}^{-2}$ term in Eq. (145) and the order- ϵ^2 term in Eq. (146) produces the double logarithmic term $\left[\frac{\log^2(1-z)}{1-z} \right]_+$. This threshold double logarithm is associated with the singular contribution in the anomalous dimension of $S_{{}^3P^{[8]}}(z)$ that is proportional to $\left[\frac{\log(1-z)}{1-z} \right]_+$, which comes from the $\epsilon_{\text{UV}}^{-2}$ term in Eq. (145) and the order- ϵ term in Eq. (146). Equivalently, the singular contribution in the anomalous dimension can also be obtained from the $\epsilon_{\text{UV}}^{-1} \log \mu^2$ term in Eq. (145) and the order- ϵ term in Eq. (146). The IR pole in Eq. (146) produces mixed poles like $1/(\epsilon_{\text{IR}} \epsilon_{\text{UV}}^2)$, which will cancel when we consider the mixing between the ${}^3S_1^{[8]}$ and ${}^3P_J^{[8]}$ states, similarly to the tree-level result. Since the most singular term in the ${}^3S_1^{[8]}$ soft function at NLO is proportional to $\left[\frac{\log(1-z)}{1-z} \right]_+$, this does not affect the double logarithmic term in the ${}^3P^{[8]}$ soft function. If we collect only the most

⁴ If we trace back the origin of the $\epsilon_{\text{UV}}^{-2}$ contribution and keep all the ϵ -dependent gamma functions, which amounts to the replacement $\epsilon_{\text{UV}}^{-2} \rightarrow \Gamma(1+3\epsilon) \Gamma(1-\epsilon) \Gamma(\epsilon_{\text{UV}}) \Gamma(2\epsilon_{\text{UV}}) / [\Gamma(1+\epsilon) \Gamma(2+2\epsilon)]$, the γ_E does not appear in the expansion in powers of ϵ , as is usual in the calculation in the $\overline{\text{MS}}$ scheme.

singular terms at each order in α_s , $S_{3P^{[8]}}(z)$ is given at NLO accuracy by

$$\begin{aligned} S_{3P^{[8]}}(z)|_{\text{threshold}} &= \frac{(N_c^2 - 4)(N_c^2 - 1)}{N_c} \frac{1}{\pi m^2 P^+} \left\{ -\frac{1}{(1-z)_+} \right. \\ &\quad + \frac{\alpha_s C_A}{\pi} \left[4 \left(\frac{\log^2(1-z)}{1-z} \right)_+ \right. \\ &\quad \left. \left. + \frac{1}{\epsilon_{\text{UV}}} \left(\frac{-2 \log(1-z)}{1-z} \right)_+ + \frac{1}{2\epsilon_{\text{UV}}^2} \frac{1}{(1-z)_+} \right] + O(\alpha_s^2) \right\}, \end{aligned} \quad (147)$$

whose Mellin transform is

$$\begin{aligned} \tilde{S}_{3P^{[8]}}(N)|_{\text{threshold}} &= \frac{(N_c^2 - 4)(N_c^2 - 1)}{N_c} \frac{1}{\pi m^2 P^+} \left[-\log N \right. \\ &\quad \left. + \frac{\alpha_s C_A}{\pi} \left(\frac{4}{3} \log^3 N - \frac{\log^2 N}{\epsilon_{\text{UV}}} + \frac{\log N}{2\epsilon_{\text{UV}}^2} \right) + O(\alpha_s^2) \right] \\ &= \frac{(N_c^2 - 4)(N_c^2 - 1)}{N_c} \frac{-\log N}{\pi m^2 P^+} \\ &\quad \times \left[1 + \frac{\alpha_s C_A}{\pi} \left(-\frac{4}{3} \log^2 N + \frac{\log N}{\epsilon_{\text{UV}}} - \frac{1}{2\epsilon_{\text{UV}}^2} \right) + O(\alpha_s^2) \right], \end{aligned} \quad (148)$$

at large N . If we compare with the corresponding result for $\tilde{S}_{3S_1^{[8]}}(N)$ in Eq. (114), we see that while the ${}^3P^{[8]}$ soft function has the same anomalous dimension at large N as the ${}^3S_1^{[8]}$ soft function, that is, the cusp anomalous dimension in the adjoint representation. However, the coefficient of the double logarithmic term at order ϵ^0 is different from the ${}^3S_1^{[8]}$ case; this happens because the ${}^3P^{[8]}$ soft function already has a $\log N$ behavior at leading nonvanishing order in α_s .

C. ${}^3P_J^{[1]}$

The calculation of the soft functions for the ${}^3P_J^{[1]}$ channel is very similar to the ${}^3P^{[8]}$ case. The isotropic soft function $S_{3P^{[1]}}(z)$, involves almost the same diagrams as the ${}^3P^{[8]}$ soft function, and differ only by color factors. Similarly to the leading order case, explicit calculation shows that the anisotropic soft function $S_{3P^{[1]}}^{TT}(z)$ at NLO also carries an additional factor of ϵ , so that anisotropic contribution cannot produce threshold double logarithms.

1. Isotropic contribution

Similarly to the ${}^3P^{[8]}$ case, we first consider the planar diagrams. The virtual correction to the matrix element of the operator $\mathcal{W}_\beta^b({}^3P^{[1]})$ between the vacuum and the one-gluon

state yields

$$\begin{aligned}
\langle g^{a,\alpha}(l) | \mathcal{W}_\beta^b(^3P^{[1]}) | 0 \rangle |_{\text{virtual}} &= ig^2 C_A \delta^{ab} p^\mu (l_\mu \delta_\beta^\alpha - l_\beta \delta_\mu^\alpha) \int_k \frac{-i}{k^2 + i\varepsilon} p \cdot n \frac{i}{-k \cdot n + i\varepsilon} \\
&\times \left[\left(\frac{i}{l \cdot p + i\varepsilon} \right)^2 \frac{i}{(l+k) \cdot p + i\varepsilon} + \frac{i}{l \cdot p + i\varepsilon} \left(\frac{i}{(l+k) \cdot p + i\varepsilon} \right)^2 \right]. \quad (149)
\end{aligned}$$

Apart from the overall color tensor, this is exactly the same as the same diagram for the $^3P^{[8]}$ soft function. The UV-divergent contribution of the virtual planar diagram to the soft function $S_{^3P^{[1]}}(z)$ is then given by

$$\begin{aligned}
S_{^3P^{[1]}}(z) |_{\text{virtual, UV}} &= -g^2(d-2)(N_c^2 - 1) \\
&\times C_A \int dPS_l \frac{2\pi\delta(l^+ - P^+(1-z))I(l)}{(l \cdot p)^2} + \text{c.c.}, \quad (150)
\end{aligned}$$

which is same as Eq. (122) with the replacement $(N_c^2 - 4)/N_c \rightarrow 1$ in the overall color factor. Now we consider the real planar diagram. the matrix element of the operator $\mathcal{W}_\beta^b(^3P^{[1]})$ between the vacuum and a two-gluon state from the gluon attachment on the timelike Wilson line is given by

$$\begin{aligned}
\langle g^{a_1,\mu_1}(k_1) g^{a_2,\mu_2}(k_2) | \mathcal{W}_\beta^b(^3P^{[1]}) | 0 \rangle |_{\text{real (a)}} &= -ig \left[\frac{i}{p \cdot k_1 + i\varepsilon} \left(\frac{i}{p \cdot (k_1 + k_2) + i\varepsilon} \right)^2 + \left(\frac{i}{p \cdot k_1 + i\varepsilon} \right)^2 \frac{i}{p \cdot (k_1 + k_2) + i\varepsilon} \right] \\
&\times p^\mu (k_{1\mu} \delta_\beta^{\mu_1} - k_{1\beta} \delta_\mu^{\mu_1}) p^{\mu_2} f^{a_2 a_1 b}, \quad (151)
\end{aligned}$$

and the one from the gluon attachment on the lightlike Wilson line is

$$\begin{aligned}
\langle g^{a_1,\mu_1}(k_1) g^{a_2,\mu_2}(k_2) | \mathcal{W}_\beta^{yx}(^3P^{[8]}) | 0 \rangle |_{\text{real (b)}} &= -ig \frac{i}{n \cdot k_2 + i\varepsilon} \left(\frac{i}{p \cdot k_1 + i\varepsilon} \right)^2 p^\mu (k_{1\mu} \delta_\beta^{\mu_1} - k_{1\beta} \delta_\mu^{\mu_1}) n^{\mu_2} f^{a_1 a_2 b}. \quad (152)
\end{aligned}$$

Similarly to the virtual planar diagram, these results differ from the $^3P^{[8]}$ case only by overall color tensors. The UV-divergent part of the real planar diagram is given by

$$\begin{aligned}
S_{^3P^{[1]}}(z) |_{\text{real, UV}} &= - \int dPS_{k_1} \int dPS_{k_2} 2\pi\delta(k_1^+ + k_2^+ - P^+(1-z)) \\
&\times g^2(d-2) \frac{(N_c^2 - 1)(N_c^2 - 4)}{N_c} \frac{C_A p^+}{k_2^+ (k_1 \cdot p)^2 [(k_1 + k_2) \cdot p]} + \text{c.c.}, \quad (153)
\end{aligned}$$

which is equal to Eq. (130) with the replacement $(N_c^2 - 4)/N_c \rightarrow 1$.

The UV power counting of the remaining diagrams is carried out in exactly the same way as the ${}^3P^{[8]}$ case. The double virtual diagrams also vanish in the ${}^3P^{[1]}$ case, because they are proportional to a vanishing color factor $f^{abc}\delta^{bc} = 0$. For diagrams that do not vanish trivially due to color factors, the UV power counting arguments for the ${}^3P^{[8]}$ soft function apply exactly the same way. In the doubly real diagrams, the amplitude-level diagrams 3 and 4 do not appear in the color-singlet case because the timelike Wilson lines in $S_{3P^{[1]}}(z)$ terminate at the field-strength tensors. The explicit expressions for the amplitude-level results can be obtained from the $S_{3P^{[8]}}(z)$ case by the replacements $d^{bcd} \rightarrow \delta^{bd}$ and $\delta^{yc} \rightarrow 1$. The result is that the contribution from the doubly real diagrams to $S_{3P^{[1]}}(z)$ do not involve UV divergences, except for the planar diagram. Hence, the NLO threshold double logarithm in $S_{3P^{[1]}}(z)$ is same as $S_{3P^{[8]}}(z)$, with the replacement $(N_c^2 - 4)/N_c \rightarrow 1$.

2. Anisotropic contribution

It remains to show that the anisotropic contribution $S_{3P^{[8]}}^{TT}(z)$ does not contain threshold double logarithms. The strategy of the calculation is similar to the isotropic case. The UV-divergent contribution to the virtual planar diagram involves the same one-loop integral $I(l)$, and is given by

$$S_{3P^{[1]}}^{TT}(z)|_{\text{virtual, UV}} = -g^2(N_c^2 - 1)C_A \int dPS_l \frac{2\pi\delta(l^+ - P^+(1-z))}{(l \cdot p)^2} I(l) \times \left(\frac{p^2 l_+^2 p^2 - 2p^+ l^+ l \cdot p}{p_+^2 (l \cdot p)^2} + \frac{d-2}{d-1} \right) + \text{c.c.} \quad (154)$$

Similarly to the isotropic case, the mixed double pole in $I(l)$ is canceled by the soft IR divergence in the real planar diagram, so that the contribution from the planar diagrams to $S_{3P^{[8]}}^{TT}(z)$ is given by

$$S_{3P^{[1]}}^{TT}(z)|_{\text{planar, UV}} = g^2(N_c^2 - 1)C_A \frac{\mu'^{2\epsilon}}{(4\pi)^{2-\epsilon}} \frac{2^{1-2\epsilon}(p^2)^\epsilon}{\epsilon_{\text{UV}}^2} \int dPS_l \frac{2\pi\delta(l^+ - P^+(1-z))}{(l \cdot p)^{2+2\epsilon}} \times \left(\frac{p^2 l_+^2 p^2 - 2p^+ l^+ l \cdot p}{p_+^2 (l \cdot p)^2} + \frac{d-2}{d-1} \right). \quad (155)$$

The phase-space integral is almost the same as the leading-order case, except for an additional factor of $(l \cdot p)^{-2\epsilon}$ in the integrand. The result reads

$$S_{3P^{[1]}}^{TT}(z)|_{\text{planar, UV}} = g^2 \frac{3(1-\epsilon)(1-4\epsilon)\Gamma(3\epsilon_{\text{UV}})}{2(3-2\epsilon)\Gamma(4+2\epsilon)} \frac{\mu'^{2\epsilon}}{\pi^{3-2\epsilon} P^+(p^2)^{1+2\epsilon}} \frac{1}{(1-z)^{1+4\epsilon}}. \quad (156)$$

Hence, the planar diagram contribution to $S_{3P[8]}^{TT}(z)$ involves at most a single logarithm.

As was in the isotropic contribution, the doubly virtual diagrams vanish for the anisotropic contribution, as $S_{3P[1]}^{TT}(z)$ involves the same color tensor as $S_{3P[1]}(z)$, they are proportional to a vanishing color factor. Similarly to the calculation of the planar diagram, the virtual-real diagram contributions to $S_{3P[1]}^{TT}(z)$ always involve an explicit factor of ϵ , which renders the single-UV poles in the virtual one-loop diagrams finite. The doubly real diagrams need calculation, which can be done by using the amplitude-level results for $S_{3P[8]}(z)$ with the replacements $d^{bcd} \rightarrow \delta^{bd}$ and $\delta^{yc} \rightarrow 1$. By explicit calculation, we find that the potentially UV-divergent integrals that appear in the doubly real diagrams for $S_{3P[1]}^{TT}(z)$ are the same ones that appeared in $S_{3P[8]}(z)$, which are in fact UV finite. Hence, the only UV-divergent contributions to $S_{3P[1]}^{TT}(z)$ come from the planar diagrams, which only produce single logarithms.

3. Results and discussion

As we have shown by explicit calculation, the threshold double logarithm in the isotropic contribution $S_{3P[1]}(z)$ is equal to the $S_{3P[8]}(z)$, with the replacement $(N_c^2 - 4)/N_c \rightarrow 1$ in the overall color factor. Thus if we collect only the contributions relevant for threshold double logarithms, we have

$$S_{3P[1]}(z)|_{\text{threshold}} = \frac{N_c^2 - 1}{\pi m^2 P^+} \left\{ -\frac{1}{(1-z)_+} + \frac{\alpha_s C_A}{\pi} \left[4 \left(\frac{\log^2(1-z)}{1-z} \right)_+ + \frac{1}{\epsilon_{\text{UV}}} \left(\frac{-2 \log(1-z)}{1-z} \right)_+ + \frac{1}{2\epsilon_{\text{UV}}^2} \frac{1}{(1-z)_+} \right] + O(\alpha_s^2) \right\}, \quad (157)$$

whose Mellin transform is

$$\tilde{S}_{3P[1]}(N)|_{\text{threshold}} = \frac{N_c^2 - 1}{\pi m^2 P^+} (-\log N) \times \left[1 + \frac{\alpha_s C_A}{\pi} \left(-\frac{4}{3} \log^2 N + \frac{\log N}{\epsilon_{\text{UV}}} - \frac{1}{2\epsilon_{\text{UV}}^2} \right) + O(\alpha_s^2) \right]. \quad (158)$$

The anisotropic contribution $S_{3P[1]}^{TT}(z)$ does not contain threshold double logarithms, because the NLO correction only involves single UV poles. This implies that the coefficient of the threshold double logarithmic correction factor in the ${}^3P_J^{[1]}$ fragmentation functions are independent of the total spin J of the $Q\bar{Q}$ state, as was found in the explicit calculation of the fragmentation function at NLO in Ref. [18]. We also expect that, from the soft factorization

of polarized ${}^3P_J^{[1]}$ fragmentation functions, that the threshold double logarithmic correction factor is also independent of the $Q\bar{Q}$ helicity.

The calculation of the isotropic soft function $S_{3P^{[1]}}(z)$ can be checked against the calculation in Ref. [44]. The calculation Ref. [44] at leading nonvanishing power in the expansion in q , corresponds to the first moment of the isotropic soft function $\tilde{S}_{3P^{[1]}}(N = 1) = \int_0^1 dz S_{3P^{[1]}}(z)$. The sum of diagrams \mathcal{C} and \mathcal{D} in Ref. [44] corresponds to the contribution from the planar diagrams in this work. In Ref. [44], the UV divergences in the phase-space integral have been regulated by using a cutoff, while the remaining UV divergences are regulated dimensionally. This approach was used in Ref. [44] because the aim was to isolate the IR divergences in the NRQCD LDMEs; otherwise, the diagrams would have vanished due to the scaleless nature of loop corrections to NRQCD LDMEs. This makes it easier for us to compare the results between Ref. [44] and our calculation of $S_{3P^{[1]}}(z)$. In Ref. [44], it was found that only the diagrams \mathcal{C} and \mathcal{D} contained double UV poles, consistently with our results for planar diagrams. The vanishing of diagrams \mathcal{A} and \mathcal{B} , as well as the non-appearance of UV divergences in diagrams \mathcal{E} and \mathcal{F} in Ref. [44] are also consistent with our analysis of non-planar diagrams.

D. Summary of NLO results

The results for the threshold behavior of the NLO calculations of the soft functions are shown in Eqs. (114), (148), and (158) for the ${}^3S_1^{[8]}$, ${}^3P^{[8]}$, and ${}^3P_J^{[1]}$ channels, respectively. The large- N behavior of the results can be written in the form

$$\tilde{S}_{3S_1^{[8]}}(N)|_{\text{threshold}} = \left[1 + \frac{\alpha_s C_A}{\pi} \left(-\log^2 N + \frac{\log N}{\epsilon_{\text{UV}}} - \frac{1}{2\epsilon_{\text{UV}}^2} \right) + O(\alpha_s^2) \right] \tilde{S}_{3S_1^{[8]}}^{\text{LO}}(N), \quad (159a)$$

$$\tilde{S}_{3P^{[8]}}(N)|_{\text{threshold}} = \left[1 + \frac{\alpha_s C_A}{\pi} \left(-\frac{4}{3} \log^2 N + \frac{\log N}{\epsilon_{\text{UV}}} - \frac{1}{2\epsilon_{\text{UV}}^2} \right) + O(\alpha_s^2) \right] \tilde{S}_{3P^{[8]}}^{\text{LO}}(N), \quad (159b)$$

$$\tilde{S}_{3P^{[1]}}(N)|_{\text{threshold}} = \left[1 + \frac{\alpha_s C_A}{\pi} \left(-\frac{4}{3} \log^2 N + \frac{\log N}{\epsilon_{\text{UV}}} - \frac{1}{2\epsilon_{\text{UV}}^2} \right) + O(\alpha_s^2) \right] \tilde{S}_{3P^{[1]}}^{\text{LO}}(N). \quad (159c)$$

Since $C_A = N_c$, the NLO finite pieces exactly reproduce the threshold double logarithms in the FFs given in Eq. (15). The single pole term is exactly the large- N behavior of the Mellin transform of the $2C_A z/(1-z)_+$ term in the gluon splitting function $P_{gg}(z)$. The double pole $1/\epsilon_{\text{UV}}^2$, which does not depend on N or the final state, can be absorbed into the NLO Wilson coefficient of the soft factorization formula. The universality of the single and

double pole terms imply that the threshold double logarithms come from a single universal origin, namely, the cusp anomalous dimension that gives rise to the $2C_A z/(1-z)_+$ term in $P_{gg}(z)$. However, unlike the pole terms the coefficients of the $\log^2 N$ term depend on the channel; because the threshold double logarithm is associated with an infrared divergence, its coefficient depends on the final state.

VI. RESUMMATION

Since the threshold double logarithm always occurs from the planar diagram, the resummation is straightforward; an exchange of a gluon with momentum l between the timelike and lightlike Wilson lines implies a loss of quarkonium momentum by l , or equivalently, an increase in the momentum of the fragmenting gluon by l . Thus, the effect of adding this gluon exchange to the tree-level soft function $S_{\mathcal{N}}^{\text{LO}}(z)$ for channel \mathcal{N} can be written in the form

$$\int_0^{K^+(1-z)} \frac{dl^+}{l^+} \mathcal{K}(l^+) [S_{\mathcal{N}}^{\text{LO}}(z + l^+/K^+) - S_{\mathcal{N}}^{\text{LO}}(z)], \quad (160)$$

where $\mathcal{K}(l^+)$ is a kernel that can be determined from explicit calculation of the gluon exchange diagram. The subtraction term $-S_{\mathcal{N}}^{\text{LO}}(z)$ subtracts the $l^+ = 0$ singularity so that only the finite piece remains in Eq. (160). By using change of variables, this integral can be rewritten as a convolution integral that is diagonalized in Mellin space. We define z' through $z/z' \equiv z + l^+/K^+$, so that Eq. (160) can be rewritten as

$$\int_0^z \frac{dz'}{z'} \left[\frac{\mathcal{K}(P^+(1-z')/z')}{1-z'} \right]_+ S_{\mathcal{N}}^{\text{LO}}(z/z') = \left[\frac{\mathcal{K}(P^+(1-z)/z)}{1-z} \right]_+ \otimes S_{\mathcal{N}}^{\text{LO}}(z). \quad (161)$$

From our NLO calculation of the soft functions we can identify the Mellin transform of the kernel $[\mathcal{K}(P^+(1-z)/z)/(1-z)]_+$ as

$$J_{^3S_1^{[8]}}^N = \frac{\alpha_s C_A}{\pi} \int_0^1 \frac{dz}{z} z^N \left[\frac{-2 \log(1-z)}{1-z} \right]_+, \quad (162)$$

for the $^3S_1^{[8]}$ channel, and

$$J_{^3P^{[8]}}^N = \frac{4\alpha_s C_A}{3\pi} \int_0^1 \frac{dz}{z} z^N \left[\frac{-2 \log(1-z)}{1-z} \right]_+, \quad (163)$$

$$J_{^3P^{[1]}}^N = \frac{4\alpha_s C_A}{3\pi} \int_0^1 \frac{dz}{z} z^N \left[\frac{-2 \log(1-z)}{1-z} \right]_+, \quad (164)$$

for the ${}^3P^{[8]}$ and ${}^3P^{[1]}$ channels. Note that $J_{{}^3P^{[8]}}^N = J_{{}^3P^{[1]}}^N = \frac{4}{3} J_{{}^3S_1^{[8]}}^N$, and at large N , $J_{{}^3S_1^{[8]}}^N \sim -\frac{\alpha_s C_A}{\pi} \log^2 N$. These expressions follow from the identities

$$\left[\frac{-2 \log(1-z)}{1-z} \right]_+ \otimes \delta(1-z) = \left[\frac{-2 \log(1-z)}{1-z} \right]_+, \quad (165)$$

$$\begin{aligned} \left[\frac{-2 \log(1-z)}{1-z} \right]_+ \otimes \frac{1}{(1-z)_+} &= \left[\frac{3 \log^2(1-z)}{1-z} \right]_+ - \frac{\pi^2}{3} \frac{1}{(1-z)_+} \\ &\quad + 2\zeta(3)\delta(1-z) + \frac{2 \log z \log(1-z)}{1-z}. \end{aligned} \quad (166)$$

It is straightforward to generalize this result to a ladder of an arbitrary number insertions of planar gluons. Because the insertions of planar gluons onto the temporal Wilson line are time ordered, in Mellin space the gluon insertions exponentiate in the form [47]

$$\tilde{S}_{\mathcal{N}}^{\text{resum}}(N) = \exp [J_{\mathcal{N}}^N] \tilde{S}_{\mathcal{N}}^{\text{LO}}(N). \quad (167)$$

Since the $z \rightarrow 1$ behavior of the fragmentation function is contained in the soft function, the same expression holds for $D^{\text{LO}}(z)$.

$$\tilde{D}_{g \rightarrow Q\bar{Q}(\mathcal{N})}^{\text{resum}}(N) = \exp [J_{\mathcal{N}}^N] \tilde{D}_{g \rightarrow Q\bar{Q}(\mathcal{N})}^{\text{LO}}(N). \quad (168)$$

This expression contains all of the leading double threshold logarithms $\tilde{D}_{g \rightarrow Q\bar{Q}(\mathcal{N})}^{\text{LO}}(N) \times \alpha_s^n \log^{2n} N$ in the all-orders result for the fragmentation function, while at leading order in α_s coincides with $\tilde{D}_{g \rightarrow Q\bar{Q}(\mathcal{N})}^{\text{LO}}(N)$. We can also combine the NLO correction term in the fixed-order calculation of the fragmentation function to obtain the expression

$$\tilde{D}_{g \rightarrow Q\bar{Q}(\mathcal{N})}^{\text{FO+resum}}(N) = \exp [J_{\mathcal{N}}^N] \left(\tilde{D}_{g \rightarrow Q\bar{Q}(\mathcal{N})}^{\text{FO}}(N) - J_{\mathcal{N}}^N \tilde{D}_{g \rightarrow Q\bar{Q}(\mathcal{N})}^{\text{LO}}(N) \right), \quad (169)$$

where $\tilde{D}_{\mathcal{N}}^{\text{FO}}(N)$ is the fixed-order fragmentation function computed to NLO in α_s , while the last term in the parenthesis subtracts the NLO double logarithm in the fixed-order result to avoid double counting. In both Eqs. (168) and (169), the Mellin-space formulas for resummed fragmentation functions vanish as $N \rightarrow \infty$, because the factor $\exp [J_{\mathcal{N}}^N]$ vanishes faster than any power of N . As a result, the resummed fragmentation functions in z space are regular functions that vanish at $z = 1$.

Note that there is some freedom in choosing the exact form of the Mellin-space kernel $J_{\mathcal{N}}^N$. Since we are only interested in resumming the leading double threshold logarithms, any form that has the same double logarithmic large N behavior will reproduce the $\tilde{D}_{g \rightarrow Q\bar{Q}(\mathcal{N})}^{\text{LO}}(N) \times$

$\alpha_s^n \log^{2n} N$ terms in the resummed expression. The form that we choose is similar to the one that is commonly used in the Mellin-space resummation of threshold logarithms in perturbative QCD calculations; it has the advantage that the z -space expression for the kernel $J_{\mathcal{N}}^N$ vanishes quickly as $z \rightarrow 0$, so that only the behavior of the fragmentation function near the threshold $z = 1$ is affected by resummation. It also preserves the total fragmenting probability $\int_0^1 dz D(z)$, because $J_{\mathcal{N}}^N$ vanishes at $N = 1$.

Our resummation formula in Eq. (169) differs from the usual ones found in literature in that we do not formulate it as a solution of an evolution equation (see, for example, Refs. [48–51]). In the usual treatment of threshold logarithms, resummation is carried out by evolving the renormalization scale of the fragmentation function from a z -dependent scale $\mu_i = \mu_0(1 - z)$ to a z -independent fixed scale $\mu_f = \mu_0$. This is not suitable for the fragmentation functions we consider in this work, because the $D_{g \rightarrow Q\bar{Q}(\mathcal{N})}(z)$ that we compute are NRQCD short-distance coefficients that are determined through perturbative matching at the hard scale, while physics below the scale of the heavy quark mass are contained in the NRQCD long-distance matrix elements. Computing the fragmentation function at a z -dependent renormalization scale is thus inconsistent with the perturbative matching procedure. Instead, our resummation formula in Eq. (169) allows resummation of threshold logarithms while working at a fixed hard scale, consistently with the perturbative matching procedure in NRQCD.

The resummation formula in Eq. (169) first appeared in Ref. [24], which was used to explain the large- p_T measurement of prompt J/ψ production rates in Ref. [23]. One unexpected consequence of the resummation formula that was found in Ref. [24] is that the vanishing of the resummed FFs at the threshold $z = 1$ brings in reduction of the sizes of the individual SDCs $d\sigma_{Q\bar{Q}(\mathcal{N})}$ for the color-octet channels. Because of this, the strong sensitivity on the color-octet matrix elements of the quarkonium production rates computed in the NRQCD factorization formalism is fairly reduced. This is evident in the calculation of $\chi_{c1}(3872)$ production rates in Ref. [52], based on the hypothesis that it is a hidden-heavy tetraquark where the $c\bar{c}$ are mostly in the ${}^3S_1^{[8]}$ state [53–55]. In Ref. [52] it was found that it is necessary to use the resummed SDCs in order to explain the prompt $\chi_{c1}(3872)$ production rates at the LHC, as the fixed-order calculation leads to a overestimation of the cross sections, especially when compared to the non-prompt production rate. In Refs. [56, 57], resummed FFs were used to compute the transverse momentum distributions of J/ψ and

$\psi(2S)$ within jets. Use of the resummed FFs in Eq. (169) is crucial in calculations of momentum distributions, as without resummation it is not possible to obtain smooth distributions that are well behaved all the way up to the threshold $z = 1$.

VII. CONCLUSIONS

In this paper, we presented an all-orders analysis of threshold double logarithms that appear in quarkonium fragmentation functions in the nonrelativistic QCD factorization formalism. As is known from existing calculations, fixed-order calculations of quarkonium fragmentation functions involve singularities at the kinematical threshold due to emission of soft gluons, with the strongest singularities coming from the threshold double logarithms. While these singularities are integrable, this makes it impossible to ensure the positivity of quarkonium production rates in fixed-order perturbation theory, because in this case the fragmentation functions can never be positive definite for any choice of nonperturbative NRQCD matrix elements. This problem can only be resolved by resumming the threshold double logarithms to all orders in perturbation theory.

Resummation of threshold double logarithms can be carried out through soft factorization, which helps identify and isolate the source of threshold singularities. This procedure, which is based on standard methods of factorization in perturbative QCD, is discussed in detail in Sec. III. Calculation of the soft functions at leading and next-to-leading orders in the strong coupling are shown in Sec. IV and Sec. V, respectively. Through these calculations we showed that the threshold singularities in the fragmentation functions are indeed completely contained in the soft functions, and the threshold double logarithms can only arise from a specific type of planar diagram. As shown in Sec. VI, this allows us to resum the threshold double logarithms to all orders in the strong coupling, in a similar manner as the usual resummation of Sudakov double logarithms. While the result for the resummed fragmentation function was first presented in an earlier publication in Ref. [24], the detailed derivation and calculation of the soft function is shown here for the first time. The analysis presented in this work also makes it clear that the resummation formula for quarkonium fragmentation functions also applies to polarized fragmentation functions, which was argued without proof in Ref. [24].

As was shown in Ref. [24], only after threshold double logarithms are resummed to all

orders is it possible to construct quarkonium fragmentation functions that are positive definite. This is integral in establishing a proper description of prompt J/ψ production rates at very large transverse momentum. The calculation presented in this work provides the detailed derivation of the resummation formalism used in Ref. [24]. The use of resummed fragmentation functions was crucial in phenomenological studies of large- p_T production rates of J/ψ in Ref. [24], prompt production rates of $\chi_{c1}(3872)$ in Ref. [52], and the transverse momentum distribution of J/ψ and $\psi(2S)$ in jets in Refs. [56, 57].

While the problem of singularities in quarkonium fragmentation functions is essentially resolved by resumming threshold logarithms at leading double logarithmic level, the accuracy of resummation may be improved by computing the soft functions at single pole level, and also at higher orders in the strong coupling. Currently the calculation at single-pole accuracy has only been done for the ${}^3S_1^{[8]}$ channel, due to complications involving rapidity divergences that appear in the ${}^3P^{[8]}$ and ${}^3P_J^{[1]}$ channels. It may also be interesting to extend the resummation formalism to next-to-leading power in the $1/N$ expansion; such an analysis may be useful in resolving the poor convergence of the velocity expansion in the color-singlet channel, where the fragmentation functions are finite but nonzero at threshold [31, 33].

Appendix A: Mellin transform

In this appendix we collect useful formulas on Mellin transforms that we use throughout this paper. We define the Mellin transform of a function f by

$$\tilde{f}(N) = \int_0^1 \frac{dz}{z} z^N f(z). \quad (\text{A1})$$

While in the general theory of Mellin transforms the upper limit of integration is $+\infty$, in this work we will only deal with functions that vanish outside the kinematically allowed region $0 \leq z \leq 1$, so that throughout this paper the upper limit of the z integration is always 1. The Mellin transform diagonalizes the convolution

$$\int_0^1 \frac{dz}{z} z^N (f \otimes g)(z) = \tilde{f}(N) \tilde{g}(N), \quad (\text{A2})$$

where \otimes is defined by

$$(f \otimes g)(z) = \int_z^1 \frac{dz'}{z'} f(z') g(z/z'). \quad (\text{A3})$$

The original function $f(z)$ can be restored from $\tilde{f}(N)$ through the inverse Mellin transform

$$f(z) = \int_{c-i\infty}^{c+i\infty} \frac{dN}{2\pi i} z^{-N} \tilde{f}(N), \quad (\text{A4})$$

where c is chosen so that all poles of $\tilde{f}(N)$ are on the left of the integration contour. It is evident that $\tilde{f}(N)$ must vanish faster than $1/N$ as $N \rightarrow \infty$ for the contour integral to be well defined at $z = 1$. If $\tilde{f}(N)$ decreases like $1/N$, $f(z)$ at $z = 1$ can still be found by the limit $z \rightarrow 1^-$, and the inverse transform still gives a continuous function of z . However, if $\tilde{f}(N)$ does not vanish as $N \rightarrow \infty$, the inverse Mellin transform instead defines a distribution that is singular at $z = 1$. We list below the Mellin transforms of distributions that appear in this paper:

$$\int_0^1 \frac{dz}{z} z^N \delta(1-z) = 1, \quad (\text{A5a})$$

$$\int_0^1 \frac{dz}{z} z^N \frac{1}{(1-z)_+} = -H_{N-1}, \quad (\text{A5b})$$

$$\int_0^1 \frac{dz}{z} z^N \left[\frac{\log(1-z)}{1-z} \right]_+ = +\frac{1}{2} H_{N-1}^2 - \frac{1}{2} \psi^{(1)}(N) + \frac{\pi^2}{12}, \quad (\text{A5c})$$

$$\begin{aligned} \int_0^1 \frac{dz}{z} z^N \left[\frac{\log^2(1-z)}{1-z} \right]_+ &= -\frac{1}{3} H_{N-1}^3 - \frac{\pi^2}{6} H_{N-1} + H_{N-1} \psi^{(1)}(N) \\ &\quad - \frac{1}{3} \psi^{(2)}(N) - \frac{2}{3} \zeta(3), \end{aligned} \quad (\text{A5d})$$

where $H_N = \psi(N+1) + \gamma_E$ is the harmonic number, $\psi(z) = \Gamma'(z)/\Gamma(z)$ is the digamma function, γ_E is the Euler-Mascheroni constant, and $\psi^{(n)}(z) = \frac{d^n}{dz^n} \psi(z)$ is the polygamma function. From the large- z asymptotic behavior of the digamma function $\psi(z) \sim \log z$, we obtain the large- N asymptotic behaviors of the plus distributions in Mellin space given by

$$\int_0^1 \frac{dz}{z} z^N \left[\frac{\log^{m-1}(1-z)}{1-z} \right]_+ \sim \frac{(-1)^m}{m} \log^m N, \quad (\text{A6})$$

for $m = 1, 2, 3 \dots$

Appendix B: Helicity decomposition for ${}^3P_J^{[1]}$ FFs

The polarized ${}^3P_J^{[1]}$ gluon FFs have first been computed in Ref. [41] in cutoff regularization. These results can be translated to dimensional regularization based on the method

developed in Ref. [30]. We obtain

$$D_{g \rightarrow Q\bar{Q}(^3P_{J,h}^{[1]})}^{\text{soft}}(z) = \frac{4\alpha_s^2}{3(d-1)m^5N_c^2} \left[\left(\frac{Q_{J,h}}{2J+1} - a_{J,h} \log \frac{\mu_\Lambda}{2m} \right) \delta(1-z) + \frac{a_{J,h}}{(1-z)_+} + \frac{P_J^h(z)}{2J+1} \right] + O(\alpha_s^3), \quad (\text{B1})$$

where

$$a_{1,0} = a_{1,1} + a_{1,-1} = \frac{1}{2}, \quad (\text{B2a})$$

$$\frac{Q_{1,0}}{3} = \frac{1}{8}, \quad \frac{Q_{1,1} + Q_{1,-1}}{3} = 0, \quad (\text{B2b})$$

$$a_{2,0} = \frac{1}{10}, \quad a_{2,1} + a_{2,-1} = \frac{3}{10}, \quad a_{2,2} + a_{2,-2} = \frac{3}{5}, \quad (\text{B2c})$$

$$\frac{Q_{2,0}}{5} = \frac{1}{40}, \quad \frac{Q_{2,1} + Q_{2,-1}}{5} = 0, \quad \frac{Q_{2,2} + Q_{2,-2}}{5} = \frac{3}{20}, \quad (\text{B2d})$$

$$\frac{P_1^0(z)}{3} = -\frac{z}{4} - \frac{z^2}{2}, \quad \frac{P_1^1(z) + P_1^{-1}(z)}{3} = -\frac{z^2}{2}, \quad (\text{B2e})$$

$$\begin{aligned} \frac{P_2^0(z)}{5} = & -\frac{1}{20z^4} [z(2z^5 + 5z^4 + 36z^3 - 468z^2 + 864z - 432) \\ & + 216(z-2)(z-1)^2 \log(1-z)], \end{aligned} \quad (\text{B2f})$$

$$\begin{aligned} \frac{P_2^1(z) + P_2^{-1}(z)}{5} = & -\frac{3}{10z^4} [z(z^5 + 4z^4 - 56z^3 + 152z^2 - 192z + 96) \\ & + 24(z^4 - 5z^3 + 10z^2 - 10z + 4) \log(1-z)], \end{aligned} \quad (\text{B2g})$$

$$\begin{aligned} \frac{P_2^2(z) + P_2^{-2}(z)}{5} = & -\frac{3}{5z^4} [z(z^5 - 7z^4 + 25z^3 - 37z^2 + 24z - 12) \\ & + 3(z^5 - 6z^4 + 14z^3 - 16z^2 + 10z - 4) \log(1-z)]. \end{aligned} \quad (\text{B2h})$$

These expressions agree with the results shown in Ref. [39].

Appendix C: Light-cone coordinates

We use the following definition for light-cone coordinates

$$a_\pm = a^\pm = \frac{1}{\sqrt{2}}(a^0 \pm a^3), \quad (\text{C1})$$

so that

$$a \cdot b = a^+ b^- + a^- b^+ - \mathbf{a}_\perp \cdot \mathbf{b}_\perp. \quad (\text{C2})$$

The d -dimensional integral is given by

$$\int d^d k = \int_{-\infty}^{+\infty} dk^+ \int_{-\infty}^{+\infty} dk^- \int d^{d-2} k_\perp. \quad (\text{C3})$$

The k_\perp integral can be computed by using

$$\int d^{d-2} k_\perp = \frac{2\pi^{\frac{d-2}{2}}}{\Gamma(\frac{d-2}{2})} \int_0^\infty |\mathbf{k}_\perp|^{d-3} d|\mathbf{k}_\perp| = \frac{2\pi^{1-\epsilon}}{\Gamma(1-\epsilon)} \int_0^\infty |\mathbf{k}_\perp|^{1-2\epsilon} d|\mathbf{k}_\perp| \quad (\text{C4})$$

for $d = 4 - 2\epsilon$.

ACKNOWLEDGMENTS

We thank Geoffrey Bodwin for fruitful discussions on resummation of threshold logarithms. The work of H. S. C. is supported by the Basic Science Research Program through the National Research Foundation of Korea (NRF) funded by the Ministry of Education (Grant No. RS-2023-00248313) and a Korea University grant. This work is also supported in part by the National Research Foundation of Korea (NRF) under Grant Nos. RS-2025-24222969 (J. L.) and RS-2025-24533579 (U-R. K.).

All authors contributed equally to this work.

[1] J. Kodaira and L. Trentadue, Summing Soft Emission in QCD, *Phys. Lett. B* **112**, 66 (1982).

[2] J. Kodaira and L. Trentadue, Single Logarithm Effects in electron-Positron Annihilation, *Phys. Lett. B* **123**, 335 (1983).

[3] C. T. H. Davies, B. R. Webber, and W. J. Stirling, Drell-Yan Cross-Sections at Small Transverse Momentum, *JHEP* **1**, 095 (1984).

[4] J. C. Collins, D. E. Soper, and G. F. Sterman, Transverse Momentum Distribution in Drell-Yan Pair and W and Z Boson Production, *Nucl. Phys. B* **250**, 199 (1985).

[5] G. F. Sterman, Summation of Large Corrections to Short Distance Hadronic Cross-Sections, *Nucl. Phys. B* **281**, 310 (1987).

[6] S. Catani and L. Trentadue, Resummation of the QCD Perturbative Series for Hard Processes, *Nucl. Phys. B* **327**, 323 (1989).

[7] S. Catani and L. Trentadue, Comment on QCD exponentiation at large x, *Nucl. Phys. B* **353**, 183 (1991).

- [8] S. Catani, B. R. Webber, and G. Marchesini, QCD coherent branching and semiinclusive processes at large x, *Nucl. Phys. B* **349**, 635 (1991).
- [9] E. Laenen, J. Smith, and W. L. van Neerven, All order resummation of soft gluon contributions to heavy quark production in hadron hadron collisions, *Nucl. Phys. B* **369**, 543 (1992).
- [10] S. Catani, G. Turnock, B. R. Webber, and L. Trentadue, Thrust distribution in e+ e- annihilation, *Phys. Lett. B* **263**, 491 (1991).
- [11] S. Catani, G. Turnock, and B. R. Webber, Heavy jet mass distribution in e+ e- annihilation, *Phys. Lett. B* **272**, 368 (1991).
- [12] S. Catani, G. Turnock, and B. R. Webber, Jet broadening measures in e^+e^- annihilation, *Phys. Lett. B* **295**, 269 (1992).
- [13] S. Catani, L. Trentadue, G. Turnock, and B. R. Webber, Resummation of large logarithms in e+ e- event shape distributions, *Nucl. Phys. B* **407**, 3 (1993).
- [14] E. L. Berger and H. Contopanagos, The Perturbative resummed series for top quark production in hadron reactions, *Phys. Rev. D* **54**, 3085 (1996), arXiv:hep-ph/9603326.
- [15] S. Catani, M. L. Mangano, P. Nason, and L. Trentadue, The Resummation of soft gluons in hadronic collisions, *Nucl. Phys. B* **478**, 273 (1996), arXiv:hep-ph/9604351.
- [16] G. T. Bodwin, E. Braaten, and G. P. Lepage, Rigorous QCD analysis of inclusive annihilation and production of heavy quarkonium, *Phys. Rev. D* **51**, 1125 (1995), [Erratum: *Phys. Rev. D* 55, 5853 (1997)], arXiv:hep-ph/9407339.
- [17] E. Braaten and J. Lee, Next-to-leading order calculation of the color octet 3S(1) gluon fragmentation function for heavy quarkonium, *Nucl. Phys. B* **586**, 427 (2000), arXiv:hep-ph/0004228.
- [18] P. Zhang, C. Meng, Y.-Q. Ma, and K.-T. Chao, Gluon fragmentation into ${}^3P_J^{[1,8]}$ quark pair and test of NRQCD factorization at two-loop level, *J. High Energy Phys.* **08**, 111, arXiv:2011.04905 [hep-ph].
- [19] G. T. Bodwin, H. S. Chung, U.-R. Kim, and J. Lee, Fragmentation contributions to J/ψ production at the Tevatron and the LHC, *Phys. Rev. Lett.* **113**, 022001 (2014), arXiv:1403.3612 [hep-ph].
- [20] G. T. Bodwin, K.-T. Chao, H. S. Chung, U.-R. Kim, J. Lee, and Y.-Q. Ma, Fragmentation contributions to hadroproduction of prompt J/ψ , χ_{cJ} , and $\psi(2S)$ states, *Phys. Rev. D* **93**, 034041 (2016), arXiv:1509.07904 [hep-ph].

- [21] H. S. Chung, Resummation and renormalization of kinematical effects in inclusive P-wave quarkonium production, *J. High Energy Phys.* **07**, 007, arXiv:2303.17240 [hep-ph].
- [22] A.-P. Chen, Y.-Q. Ma, and C. Meng, Resolving negative cross section of quarkonium hadroproduction using soft gluon factorization, *Phys. Rev. D* **108**, 014003 (2023), arXiv:2304.04552 [hep-ph].
- [23] G. Aad *et al.* (ATLAS), Measurement of the production cross-section of J/ψ and $\psi(2S)$ mesons in pp collisions at $\sqrt{s} = 13$ TeV with the ATLAS detector, *Eur. Phys. J. C* **84**, 169 (2024), arXiv:2309.17177 [hep-ex].
- [24] H. S. Chung, U.-R. Kim, and J. Lee, Resummation of Threshold Double Logarithms in Hadroproduction of Heavy Quarkonium, *Phys. Rev. Lett.* **134**, 071902 (2025), arXiv:2408.04255 [hep-ph].
- [25] G. Grammer, Jr. and D. R. Yennie, Improved treatment for the infrared divergence problem in quantum electrodynamics, *Phys. Rev. D* **8**, 4332 (1973).
- [26] J. C. Collins and D. E. Soper, Parton Distribution and Decay Functions, *Nucl. Phys. B* **194**, 445 (1982).
- [27] G. C. Nayak, J.-W. Qiu, and G. Sterman, Fragmentation, NRQCD and NNLO factorization analysis in heavy quarkonium production, *Phys. Rev. D* **72**, 114012 (2005), arXiv:hep-ph/0509021.
- [28] M. Czakon, T. Generet, A. Mitov, and R. Poncelet, Identified Hadron Production at Hadron Colliders in Next-to-Next-to-Leading-Order QCD, *Phys. Rev. Lett.* **135**, 17 (2025), arXiv:2503.11489 [hep-ph].
- [29] H. S. Chung, U.-R. Kim, and J. Lee, Resummation of threshold double logarithms in inclusive production of heavy quarkonium, *PoS QCHSC24*, 135 (2025), arXiv:2501.10647 [hep-ph].
- [30] E. Braaten and Y.-Q. Chen, Dimensional regularization in quarkonium calculations, *Phys. Rev. D* **55**, 2693 (1997), arXiv:hep-ph/9610401.
- [31] G. T. Bodwin and J. Lee, Relativistic corrections to gluon fragmentation into spin triplet S wave quarkonium, *Phys. Rev. D* **69**, 054003 (2004), arXiv:hep-ph/0308016.
- [32] J. Lee, Next-to-leading order calculation of a fragmentation function in a light-cone gauge, *Phys. Rev. D* **71**, 094007 (2005), arXiv:hep-ph/0504285.
- [33] G. T. Bodwin, U.-R. Kim, and J. Lee, Higher-order relativistic corrections to gluon fragmentation into spin-triplet S-wave quarkonium, *JHEP* **11**, 020, [Erratum: *JHEP* 07, 170 (2023)],

arXiv:1208.5301 [hep-ph].

[34] Y.-Q. Ma, J.-W. Qiu, and H. Zhang, Heavy quarkonium fragmentation functions from a heavy quark pair. I. S wave, *Phys. Rev. D* **89**, 094029 (2014), arXiv:1311.7078 [hep-ph].

[35] E. Braaten and T. C. Yuan, Gluon fragmentation into heavy quarkonium, *Phys. Rev. Lett.* **71**, 1673 (1993), arXiv:hep-ph/9303205.

[36] P. Zhang, Y.-Q. Ma, Q. Chen, and K.-T. Chao, Analytical calculation for the gluon fragmentation into spin-triplet S -wave quarkonium, *Phys. Rev. D* **96**, 094016 (2017), arXiv:1708.01129 [hep-ph].

[37] P. Artoisenet and E. Braaten, Gluon fragmentation into quarkonium at next-to-leading order, *JHEP* **04**, 121, arXiv:1412.3834 [hep-ph].

[38] P. Artoisenet and E. Braaten, Gluon fragmentation into quarkonium at next-to-leading order using FKS subtraction, *JHEP* **01**, 227, arXiv:1810.02448 [hep-ph].

[39] Y.-Q. Ma, J.-W. Qiu, and H. Zhang, Fragmentation functions of polarized heavy quarkonium, *J. High Energy Phys.* **06**, 021, arXiv:1501.04556 [hep-ph].

[40] J. C. Collins and D. E. Soper, Back-To-Back Jets in QCD, *Nucl. Phys. B* **193**, 381 (1981), [Erratum: *Nucl.Phys.B* 213, 545 (1983)].

[41] P. L. Cho, M. B. Wise, and S. P. Trivedi, Gluon fragmentation into polarized charmonium, *Phys. Rev. D* **51**, R2039 (1995), arXiv:hep-ph/9408352.

[42] G. T. Bodwin, X. Garcia i Tormo, and J. Lee, Factorization in exclusive quarkonium production, *Phys. Rev. D* **81**, 114014 (2010), arXiv:1003.0061 [hep-ph].

[43] A. M. Polyakov, Gauge Fields as Rings of Glue, *Nucl. Phys. B* **164**, 171 (1980).

[44] G. T. Bodwin, H. S. Chung, J.-H. Ee, U.-R. Kim, and J. Lee, Covariant calculation of a two-loop test of nonrelativistic QCD factorization, *Phys. Rev. D* **101**, 096011 (2020), arXiv:1910.05497 [hep-ph].

[45] N. Brambilla, H. S. Chung, and A. Vairo, Inclusive Hadroproduction of P -Wave Heavy Quarkonia in Potential Nonrelativistic QCD, *Phys. Rev. Lett.* **126**, 082003 (2021), arXiv:2007.07613 [hep-ph].

[46] N. Brambilla, H. S. Chung, and A. Vairo, Inclusive production of heavy quarkonia in pNRQCD, *JHEP* **09**, 032, arXiv:2106.09417 [hep-ph].

[47] E. Laenen, G. Sterman, and W. Vogelsang, Recoil and threshold corrections in short distance cross-sections, *Phys. Rev. D* **63**, 114018 (2001), arXiv:hep-ph/0010080.

- [48] N. Kidonakis and G. F. Sterman, Resummation for QCD hard scattering, *Nucl. Phys. B* **505**, 321 (1997), arXiv:hep-ph/9705234.
- [49] N. Kidonakis, G. Oderda, and G. F. Sterman, Threshold resummation for dijet cross-sections, *Nucl. Phys. B* **525**, 299 (1998), arXiv:hep-ph/9801268.
- [50] N. Kidonakis, G. Oderda, and G. F. Sterman, Evolution of color exchange in QCD hard scattering, *Nucl. Phys. B* **531**, 365 (1998), arXiv:hep-ph/9803241.
- [51] R. Bonciani, S. Catani, M. L. Mangano, and P. Nason, Sudakov resummation of multiparton QCD cross-sections, *Phys. Lett. B* **575**, 268 (2003), arXiv:hep-ph/0307035.
- [52] W. K. Lai and H. S. Chung, Hadroproduction data support tetraquark hypothesis for $\chi_{c1}(3872)$, *Phys. Rev. D* **112**, 054005 (2025), arXiv:2505.06910 [hep-ph].
- [53] B. Grinstein, L. Maiani, and A. D. Polosa, Radiative decays of $X(3872)$ discriminate between the molecular and compact interpretations, *Phys. Rev. D* **109**, 074009 (2024), arXiv:2401.11623 [hep-ph].
- [54] E. Braaten and R. Bruschini, Exotic hidden-heavy hadrons and where to find them, *Phys. Lett. B* **863**, 139386 (2025), arXiv:2409.08002 [hep-ph].
- [55] N. Brambilla, A. Mohapatra, T. Scirpa, and A. Vairo, Nature of $\chi_{c1}(3872)$ and $T_{cc+}(3875)$, *Phys. Rev. Lett.* **135**, 131902 (2025), arXiv:2411.14306 [hep-ph].
- [56] Y. Wang, D. Kang, and H. S. Chung, NRQCD reconfronts LHCb data on quarkonium production within jets, *Phys. Rev. D* **112**, L071504 (2025), arXiv:2507.19022 [hep-ph].
- [57] Y. Wang, H. S. Chung, T. Ha, D. Kang, and U.-R. Kim, J/ψ Production Within Jets at the EIC, (2026), arXiv:2601.05530 [hep-ph].